QUANTIFYING THE EFFECTS OF CLIMATE CHANGE ON PAVEMENT PERFORMANCE PREDICTION USING AASHTOWARE PAVEMENT ME DESIGN

by

Md Shahjalal Chowdhury

A thesis

submitted in partial fulfillment

of the requirements for the degree of

Master of Science in Civil Engineering

Boise State University

August 2020

BOISE STATE UNIVERSITY GRADUATE COLLEGE

DEFENSE COMMITTEE AND FINAL READING APPROVALS

of the thesis submitted by

Md Shahjalal Chowdhury

Thesis Title: Quantifying the Effects of Climate Change on Pavement Performance Prediction Using AASHTOWare Pavement ME Design

Date of Final Oral Examination: 03 July 2020

The following individuals read and discussed the thesis submitted by student Md Shahjalal Chowdhury, and they evaluated their presentation and response to questions during the final oral examination. They found that the student passed the final oral examination.

Debakanta Mishra, Ph.D.	Chair, Supervisory Committee
Mojtaba Sadegh, Ph.D.	Co-Chair, Supervisory Committee
Bhaskar Chittoori, Ph.D.	Member, Supervisory Committee
Eshan V. Dave, Ph.D.	Member, Supervisory Committee

The final reading approval of the thesis was granted by Debakanta Mishra, Ph.D., Chair of the Supervisory Committee. The thesis was approved by the Graduate College.

DEDICATION

To my loving parents, family members and my wonderful wife for their unconditional love and support to reach my goals.

ACKNOWLEDGMENTS

I want to express my sincere gratitude to my advisor Dr. Debakanta Mishra for his continuous support and mentorship. Throughout my MS journey, Dr. Mishra has always been a great motivator who helped me in every possible way, and without his guidance, time, and persistent efforts, this thesis research would never come to an end.

I am grateful to my Co-Advisor, Dr. Mojtaba Sadegh, who came up with the idea of including the climate-related work in my thesis and guided me over the past year. I am also thankful to my thesis committee members, Dr. Bhaskar Chittoori and Dr. Eshan V. Dave, for generously agreeing to serve on my thesis committee, and for all of their valuable insights to improve the overall research quality. My gratitude goes to Dr. Wouter Brink of Applied Research Associates, who continuously helped me overcome problems related to the Pavement ME Design software. Dr. Brink was always available to patiently answer any questions I had during the course of my thesis research.

Finally, I would like to thank Md Fazle Rabbi, Md Jibon, Kody Johnson, Jenn McAtee, Beema Dahal, Mahmudul Hasan, Asif Rahman, Mostofa Najmus Sakib, Nazmul Islam, Aminul Islam, Touhidul Islam, Subroto Singha, Nuhil Mehdy, and Golam Dastogir for giving me the much-needed social support during my studies in the United States.

ABSTRACT

Climate change is one of the most concerning global issues and has the potential to influence every aspect of human life. Like different components of society, it can impose significant adverse impacts on pavement infrastructure. Although several research efforts have focused on studying the effects of climate change on natural and built systems, its impact on pavement performance has not been studied as extensively. The primary objectives of this thesis research was to quantify the effect of temperature changes on flexible pavement response and performance prediction using the AASHTOWare Pavement ME Design (PMED), and quantify the effects of Local Calibration Factors (LCFs) used by different state highway agencies in the United States on predicted pavement performance. Particular emphasis was given to LCF values used by the Idaho Transportation Department. The climatic data, as well as LCFs corresponding to several different states, were used to identify how different LCF values affect pavement performance prediction. The effects of atmospheric temperature changes on pavement temperature and Asphalt Concrete (AC) layer modulus were studied by analyzing the intermediate files generated by PMED. Finally, the impact of temperature change on AC dynamic modulus (E*) was also analyzed to link the PMED-predicted distresses with asphalt mix properties.

Historical climatic data was obtained from the Modern-Era Retrospective Analysis for Research and Applications (MERRA) database. Projected data considered to simulate the temperature changes in the future were generated by adopting two different

approaches: (1) Manual alteration of historical temperature distribution data to represent scenarios with increased mean and standard deviation values; and (2) Use of temperature data projected by established Global Climate Models (GCM). All different climatic scenarios were used in PMED along with a standard pavement section, and the distresses predicted over the design life of the pavement were compared. Simulation results showed consistent increase in Total Pavement rutting and AC rutting with increasing air temperatures. The effect of temperature increase on AC thermal cracking predicted by PMED demonstrated inconsistent trends. In contrast, the projected temperature increase had no significant effect on bottom-up fatigue cracking for the chosen study locations. It was found that the impact of changed air temperatures can be different for pavement sections constructed in different geographic locations. Moreover, the analysis confirmed that the Local Calibration Factors (LCFs) established by different state highway agencies played a major role in governing the effect of future temperature increase on predicted pavement performance. Through an extensive study of the LCFs used in the states of Idaho, Colorado, and Michigan, it was observed that the LCFs in Idaho did not adequately reflect the effects of future temperature changes on predicted pavement performance. Findings from this study emphasize the importance of considering non-stationary climate conditions likely to occur in the future during the process of pavement design. Moreover, this study also highlighted different aspects of the LCFs that play a significant role in capturing the effects of climatic factors on pavement performance predicted by PMED. Based on the findings, it is believed that further fine-tuning of the LCFs used in Idaho may be needed.

TABLE OF CONTENTS

LIST OF TABLES

LIST OF FIGURES

LIST OF ABBREVIATIONS

MEPDG	Mechanistic-Empirical Pavement Design Guide
M-E	Mechanistic-Empirical
PMED	Pavement Mechanistic-Empirical Design
IPCC	Intergovernmental Panel on Climate Change
GCFs	Global Calibration Factors
LCFs	Local Calibration Factors
GCMs	Global Climatic Models
NASA	National Aeronautics and Space Administration
CIA	Central Intelligence Agency
FHWA	Federal Highway Administration
LTPP	Long-Term Pavement Performance Program (LTPP)
AASHTO	American Association of State Highway and Transportation Officials
NCHRP	National Cooperative Highway Research Program
ARA	Applied Research Associates
MERRA	Modern-Era Retrospective Analysis for Research and Applications
MACA	Multivariate Adaptive Constructed Analogs
CMIP5	Coupled Model Inter-Comparison Project-Phase 5
RCP	Representative Concentration Pathway
WIM	Weight in Motion

CHAPTER ONE: INTRODUCTION

Climate Change

This research effort primarily focused on two broad topics: Climate change and Pavement Engineering. Climate change is one of the most concerning issues facing modern society. It causes significant adverse impacts on human as well as infrastructure health. Climate change is defined as global or regional change in any of the climatic parameters, such as precipitation, temperature, humidity, sunshine, and wind ("Climate change," n.d.; National Aeronautics and Space Administration [NASA], 2014). The subject of climate change has captured the attention of the research community for several decades. A vast number of scientific publications have addressed different aspects of climate change and the corresponding adverse effects. Although the general perception about factors driving the climate change phenomenon is not consistent across the world (Hansen et al., 2012), most researchers agree on some of the primary factors. One such factor is the increase in greenhouse gas, especially CO_2 in the atmosphere. Increased CO_2 in the atmosphere has been linked to the global rise in temperature; a phenomenon also referred to as *Global Warming*. After the industrial revolution, in the 1800s, greenhouse gas emissions and the CO_2 level in the atmosphere has increased by record amounts, attaining higher levels compared to any other time in the past 800,000 years (National Aeronautics and Space Administration [NASA], n.d.). The Fifth Assessment Report (AR5) of the Intergovernmental Panel on Climate Change (IPCC) reported that the last three decades have consecutively become warmer; and there is a 95% chance that human

activities had driven this change (Stocker et al., 2013). The AR5 also stated that in 2017, the anthropogenic temperature increase was on an average 1°C higher than its corresponding value during pre-industrial times (Allen et al., 2018). Scientists predict that unless remedial/preventive actions are taken to control global CO_2 emission levels, these trends and associated adverse impacts will continue beyond the next century. Potential regional and global effects will encompass all aspects of human life, including the transportation infrastructure (Hayhoe et al., 2008; Daniel et al., 2014). The current research effort focused on studying the effects of temperature change on flexible pavement response and performance.

Significance of the Pavement Network in the United States

The United States (U.S.) has the most extensive and longest roadway network in the world. According to the World Factbook released by the Central Intelligence Agency (CIA) (Central Intelligence Agency [CIA], n.d.), the total length of the US road network is over 4 million miles; this comprises approximately 2.7 million miles of paved roads and approximately 1.5 million miles of unpaved highway. The road network also consists of nearly fifty thousand miles of expressway. Just for the sake of comparison, the length of the entire U.S. road network is approximately 4.40% of the distance from the Earth to the Sun (92.96 million miles), 12.1% of the closest distance from the Earth to the Mars (33.9 million miles), and more than 17 times of the distance from the Earth to the Moon (2,38,900 miles). Traveling at the speed of sound (767 mph), it would take approximately five months to traverse the entire length of the paved roadway network in the US.

Moreover, according to the Bureau of Transportation Statistics (BTS), during the 2014 fiscal year, total government transport-related revenue was 183,588 million dollars,

and the total expenditure was 3,23,995 million dollars (considering the dollar value of 2014) (Bureau of Transportation Statistics [BTS], n.d.). This spending can increase even further when the road network deteriorates significantly due to external (traffic- or environment-related) factors.

Background and Problem Statement

Like any other civil engineering structure, pavements are usually designed and constructed for a specific design period with an optimum section that can withstand the traffic- and environment-induced loading throughout its design life. The lifetime of a pavement section varies depending on its type and function. The primary factors contributing to pavement distresses are aspects related to traffic and environmental loading. Generally, with time, the amount and severity of distresses in a pavement section increase, and the level of serviceability decreases. The current research focuses primarily on studying the effects of environmental factors on flexible pavement performance. In particular, emphasis is on studying the effects of temperature increases that can be attributed to prevalent patterns in climate change. In order to isolate the effects of temperature change on pavement performance, traffic loading with a 3% linear growth was considered during pavement analysis and performance prediction.

Pavement performance can be affected by multiple climatic parameters such as air temperature, precipitation, sunshine, relative humidity, wind speed, groundwater table, and number of freeze-thaw cycles. Different manifestations of climate change can adversely affect flexible pavement performance through different mechanisms. For example, higher temperatures lead to softer Asphalt Concrete (AC) layers, thereby increasing surface rutting under heavy loads. Similarly, increased precipitation can

increase the moisture content in unbound (soil and aggregate) layers, resulting in poor support conditions underneath the pavement. This can lead to rapid structural deterioration under heavy loads

In addition, the standard practice of pavement design involves the assumption of "stationary" climatic conditions. In other words, the historical climatic conditions at a particular location are assumed to remain unchanged throughout the design life of a pavement section. However, numerous research studies have proved that future climatic conditions will no longer be the same as what was observed historically, and the changed climatic conditions need to be incorporated into pavement design. Failure to account for the effects of climate change during pavement design may lead to premature failure. This would result in undesirable driving conditions for road users, ultimately requiring significant financial investments for maintenance and rehabilitation.

Underwood et al. (2017) investigated how climate change could affect the life-cycle cost of flexible pavement infrastructure. Findings from their study showed that the historical assumption of "stationary" climatic conditions greatly influences the selection of the material and the cost associated with it. They emphasized that in the past 20 years, among the 799 different U.S. locations considered, 35% had selected the wrong materials for pavement construction. Besides, they also projected that if the current practice of material selection continues based on the stationary climatic data, the changing temperature estimated from the RCP 4.5 (*R*epresentative *C*oncentration *P*athway 4.5; discussed later in this thesis) scenario will increase the pavement life-cycle cost by US$13.6, US$19.0, and US$21.8 billion by 2010, 2040, and 2070, respectively. The projected additional cost will be even higher (US$14.5, US$26.3, and US$35.8) under the

RCP 8.5 scenario. Therefore, it is important to consider the effects of future climatic conditions during the design and construction of pavement sections. The current study aimed to quantify the effect of changing temperature patterns on flexible pavement performance predicted using AASHTOWare Pavement ME Design (PMED).

Research Objective

The overall goal of this research effort was to thoroughly investigate how PMED captures the effects of climatic factors (temperature in particular) during pavement analysis and performance prediction. More specifically, the current study solely focused on evaluating the impact of changing temperature patterns in the future on flexible pavement performance. Individual research objectives were to:

1. Quantify the effects of synthetically generated future temperature distribution data on pavement response and performance prediction using PMED.

2. Assess the impact of LCF values on how PMED captures the effects of changing temperature distribution patterns while predicting pavement performance.

3. Thoroughly illustrate how different LCF values combined with varying climatic condition data can lead to significantly different pavement performance predictions.

4. Investigate how changing air temperature patterns get translated into changing pavement temperature patterns within PMED. The current study

also investigated how the changing pavement temperatures affected the AC sublayer modulus distribution within a pavement structure.

Research Approach

Two different climatic scenarios were considered during this thesis research:

(1) Historical climatic data obtained from the MERRA reanalysis dataset; and

(2) Future/projected climatic conditions represented by changing temperature distribution patterns.

Note that the first scenario is representative of current practice in the US that assumes a "stationary" climate throughout the design life of the pavement. The second scenario, on the other hand, represents changed temperature distribution in the future. These altered temperature distribution patterns for the future were generated by either manually shifting the temperature distribution to represent warmer climates in the future, or by downscaling the projected temperature distribution data from established Global Climatic Models (GCMs). Pavement performance predictions using PMED were compared under both scenarios.

The manual “shifting” of past temperature distribution patterns to represent future climatic conditions was accomplished by altering the mean (μ) and/or standard deviation (σ) of the temperature distribution data. The primary objective of this approach was to achieve a detailed understanding of the functionalities of distress prediction models inherent to PMED and how pavement distress predictions are affected by temperature changes. Accordingly, the very first step involved analysis and performance prediction of a typical flexible pavement section in Boise, Idaho, under stationary and altered temperature distribution conditions. Analyses were performed using both Global and

Local Calibration factors to investigate how changing the calibration factors affected pavement performance predictions. Another scenario modelled to study the effect of altered temperature distributions involved modifying the temperature distribution to simulate seasonal extremes. In other words, instead of altering the mean or the standard deviation value of the annual temperature distribution, only data for certain seasons was modified. This was done to simulate cases where the effects of climate change on temperature are felt predominantly in the summer or the winter seasons. Such targeted alterations in the temperature distribution would facilitate an in-depth understanding of the functionality of the distress models inherent to PMED.

Besides using the climatic data and LCFs for Boise, Idaho (BOI), the current study also focused on two more locations (Denver, Colorado or DEN, and Detroit, Michigan or DTM) during pavement performance prediction under altered temperature distributions. Simulation results obtained from those cities were compared against those for BOI, Idaho, to identify the location-based climatic impact on pavement performance prediction.

Once a basic understanding of the PMED distress prediction trends was established, the second method of simulating altered temperature distributions involved the use of downscaled temperature data from four randomly selected GCMs. Using the temperature data projected by GCMs to analyze pavement performance in the future is more realistic as those climatic models have been developed by climate scientists around the world, and temperature distributions thus projected, are more representative of plausible climatic conditions compared to artificially altered temperature distributions. The primary focus during this task was to compare pavement performances under

temperature scenarios that are likely to occur in the future and compare the performances of different LCFs in capturing the effects of the temperature changes. Note that the alterations in climatic conditions (both through manual shifting as well as through downscaling of the GCM data) in this study constituted changes in temperature distributions only; all other climatic factors (precipitation, wind speed, percent sunshine, and relative humidity) were kept unchanged (or under "stationary conditions").

Organization of the Thesis

This thesis document comprises a total of four chapters. Chapter 2 presents the background and findings from the review of previous studies related to climate change and pavement performance. Moreover, Chapter 2 also describes the data processing methods adopted in this study to generate the future temperature distributions that were subsequently used as input in PMED. Chapter 3 presents all relevant details concerning the research approach, discusses the relevant findings and corresponding implications. Finally, Chapter 4 summarizes important findings from the current research and provides recommendations for future research.

CHAPTER TWO: BACKGROUND AND LITERATURE REVIEW

Previous Research on Effects of Climate Change on Pavement Performance

Several studies over the past few years have focused on studying climate change and its effects on the pavement infrastructure. The Infrastructure & Climate Network (ICNet) at the University of New Hampshire, USA, is one of the leading research organizations in this field. ICNet researchers have evaluated the progress, challenges, and future work required to merge the disciplines of *climate change* and *transportation infrastructure* (Douglas et al., 2017). ICNet researchers have also studied topics such as the effects of Sea Level Rise on transportation design and planning, the impact of Reclaimed Asphalt Pavement (RAP) on pavement life cycle costs under future temperatures, etc. (Hayhoe et al., 2015; Knott et al., 2017; Qiao et al., 2019).

Similarly, Mallick et al., (2018) used Monte Carlo simulations of climatic data collected from two different sources and a system dynamics model to establish a framework for assessing climatic impacts on the pavement performance. Daniel et al., (2018) studied the effects of winter temperature changes on frost-thaw conditions and load restriction timings for low-volume roadways and reported that the low traffic volumes roads would deteriorate faster due to the expected changes in freeze-thaw patterns.

Stoner et al. (2019) studied the impact of future climate on flexible pavement performance and developed a method to project the hourly climate data for different locations within the U.S. Additionally, several research studies over the years have

focused on the implementation of mechanistic-empirical pavement design practices by developing databases for state-specific traffic distributions, material properties, and climatic inputs. Moreover, several research studies have focused on establishing state-specific (local) calibration factors to be used in the transfer functions (Hall et al., 2005; Darter et al., 2009; Li et al., 2013; Schwartz et al., 2015; Bayomy et al., 2018; Jibon et al., 2020). Researchers have also investigated climatic impacts on pavements in the US and abroad using PMED (Qiao et al., 2013; Elshaeb et al., 2014; Gudipudi et al., 2017; El-Maaty, 2017; Yang et al., 2017; Hasan & Tarefder, 2018).

Qiao et al. (2013) investigated the sensitivity of pavement performance to all the climatic factors, including the annual and seasonal temperature change. They observed that temperature change has a significant impact on pavement distress predictions. Similarly, Elshaeb et al. (2014) developed climatic input data for PMED to evaluate the influence of climatic factors on pavement performance in 16 locations of Egypt and observed that temperature variations had a significant impact on predicted pavement performance. Gudipudi et al. (2017) studied the effects of temperature and precipitation change on pavement performance using PMED. Different global climate models and climatic regions were considered to observe the change in pavement performance predictions due to changes incorporated into primary climate parameters. El-Maaty (2017) used PMED to observe that temperature variations at a given location had adverse impacts on flexible pavement performance in Egypt. Yang et al. (2017) used PMED to evaluate the effects of all five climatic factors on flexible pavement distress prediction at six different locations in Michigan and found that temperature was the most significant climatic factor affecting pavement performance. Hasan & Tarefder (2018) studied the

effects of mean annual temperature and precipitation on pavement performance in 13 U.S. states with varying climatic conditions. They confirmed that certain pavement distress predictions were significantly influenced by temperature, whereas several others were influenced by precipitation.

Most of the previous studies analysed the effects of temperature change on pavement performance using projected climate data obtained from GCMs. The current study, on the other hand, focused not only on investigating the effects of temperature changes on flexible pavement performance, but also the effects of different LCFs on pavement performance prediction using PMED. The objective was to understand how PMED captures the effects of temperature change using the distress prediction models. To generate altered temperature distributions representing future climatic conditions, this study adopted a statistical approach to manually modify the historical temperature distribution data.

Moreover, the effects of temperature change on different parameters such as PMED-generated pavement layer temperature and AC sub-layer modulus were also studied. This parametric analysis facilitated an in-depth understanding of PMED distress prediction trends. Subsequently, more realistic future temperature distributions were obtained from selected GCMs, and the data was downscaled to generate hourly temperature distributions that can be used as input during PMED analysis. Pavement performance prediction using the downscaled GCM data facilitated verification of the trends observed during analyses with the manually shifted data.

AASHTOWare Pavement ME Design

The AASHTOWare Pavement ME Design (PMED) software (AASHTO, 2019) is an implementation of the Mechanistic-Empirical (M-E) pavement design approach developed under the scope of *N*ational *C*ooperative *H*ighway *R*esearch *P*rogram (NCHRP) project 1-37A, (Applied Research Associates [ARA], 2004) and documented in the Mechanistic-Empirical Pavement Design Guide (MEPDG). (AASHTO, 2008). The M-E pavement design approach comprises of mechanistic and empirical components that are combined to facilitate analysis and performance prediction of pavement structures. In the mechanistic component, it relies on the principles of physics (or mechanics) to compute critical pavement response parameters (stress, strain, deflection) under traffic- as well as environment-induced loading using specified material properties. As the next step, the M-E approach uses empirical transfer functions (or damage models) to predict pavement distresses from the critical pavement response parameters. Different transfer functions are used to predict commonly observed pavement distresses; in case of flexible pavements, the primary distresses being predicted include: rutting, thermal cracking, and fatigue cracking. Additionally, PMED also predicts the pavement surface roughness using the International Roughness Index (IRI) as the quantifying measure. Details about the principle of M-E design and required inputs can be found in the NCHRP project 1-37A final report (ARA, 2004).

Figure 2.1 shows a schematic of the PMED iterative design process adopted from the Idaho PMED user's guide. (Mallela et al., 2014).

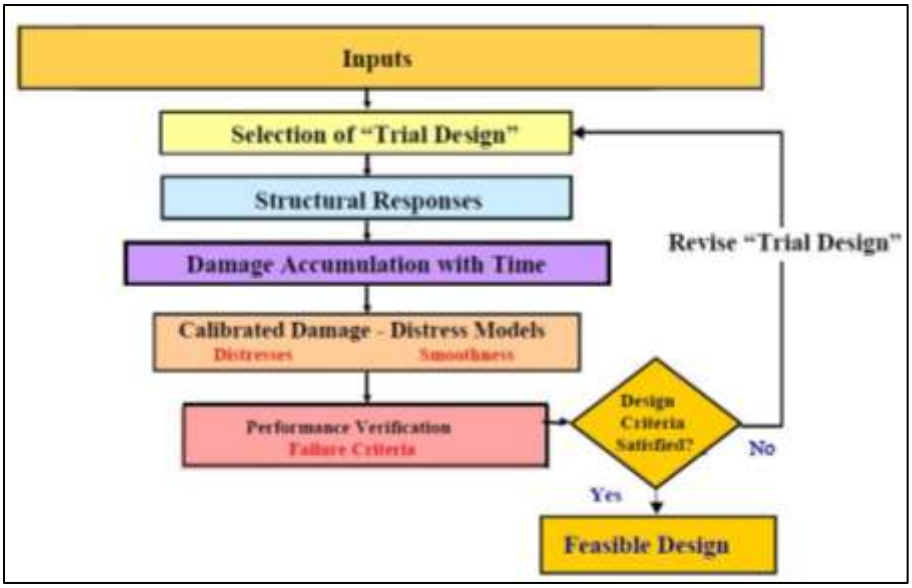

Figure 2.1 Schematic Showing the Iterative Nature Design Process in AASHTOWare Pavement ME

Tables 2.1 summarizes the transfer functions used in PMED to predict the different distress types in flexible pavements (Mallela et al., 2014). Further details of the variables associated with the transfer functions can are available in NCHRP 1-37A Final Report: Appendix GG-1, Appendix HH, and Appendix II-1 and have been excluded from this chapter for the sake of brevity (ARA, 2004).

Table 2.1 Transfer Functions used in PMED Performance Models

Distress Type	Transfer Function Formulation
AC Rutting	$\Delta p_{(AC)} = \beta_{1r} k_z \varepsilon_{r(AC)} 10^{k_{1r}} n^{k_{2r}\beta_{2r}} T^{k_{3r}\beta_{3r}} h_{ac}$
Unbound or granular or aggregate base Rutting	$\Delta p_{(soil)} = \beta_{s1} k_{s1} \varepsilon_v h_{soil} \left(\frac{\varepsilon_0}{\varepsilon_r}\right) e^{-\left(\frac{\rho}{n}\right)^{\beta}}$
Subgrade rutting	
Bottom-up fatigue cracking (Alligator cracking)	$FC_{Bottom} = \left(\frac{1}{60}\right)\left(\frac{c_4}{1 + e^{\left(c_1 c_1^* + c_2 c_2^* Log(DI_{Bottom} * 100)\right)}}\right)$
Top-down fatigue cracking (Longitudinal cracking)	$FC_{Top} = 10.56\left(\frac{c_4}{1 + e^{\left(c_1 - c_2 Log(DI_{Top})\right)}}\right)$
Thermal cracking (transverse cracking)	$TC = \beta_{t1} N \left[\frac{1}{\sigma_d} Log\left(\frac{c_d}{H_{AC}}\right)\right]$
IRI	$IRI = IRI_o + C_1(RD) + C_2(FC_{Total}) + C_3(TC) + C_4(SF)$

As seen from Table 2.1**,** the transfer functions comprise multiple coefficients, whose values are established through statistical regression of empirical data. The values of these model coefficients can be significantly affected by local conditions, therefore, requiring local PMED calibration efforts by state highway agencies. It is important to note that during the original MEPDG developmental effort, "global" values (known as Global Calibration Factors or GCFs) of the model coefficients were established using national-level empirical data. A large volume of actual pavement section data corresponding to different pavement types, materials properties, and climatic conditions across the USA was collected mostly through the Federal Highway Administration (FHWA) Long-Term Pavement Performance Program (LTPP) and other State or Local agencies to calibrate the PMED. However, it was not possible to account for all the data

variability related to the candidate locations and include the data for all types of pavement in the PMED.

To further improve the accuracy of these models in predicting pavement performance in a particular geographic region, the models need to be further "fine-tuned" using Local Calibration Factors (LCFs). For example, in the AC rutting transfer function (refer to Table 2.1), the $k_{1,2,3}$ terms represent GCFs, whereas the $\beta_{1,2,3}$ terms represent LCFs. The GCFs for all the transfer functions of all the PMED prediction models were developed through the NCHRP 1-37A project (ARA, 2004), and were later recalibrated through NCHRP Project 1-40D (Darter et al., 2006). However, during this national level calibration effort, it was not possible to calibrate the models based on state-specific data.

Therefore, to further improve the accuracy of these models in predicting pavement performance in a particular geographic region, the models need to be further "fine-tuned" using Local Calibration Factors (LCFs). LCFs are established by State and Local agencies to minimize the impact of data variability in performance predictions and to incorporate the actual local conditions of the candidate location. A large number of states have already established LCFs based on the procedures outlined by the American Association of State Highway and Transportation Officials (AASHTO) (AASHTO, 2010). For example, in the AC rutting transfer function (refer to Table 2.1), the $k_{1,2,3}$ terms represent the GCFs, whereas the $\beta_{1,2,3}$ terms represent the LCFs.

As previously mentioned, the current study focused on comparing the LCFs for three different states (Idaho, Colorado, and Michigan). Table 2.2 lists the GCFs established through NCHRP 1-40D project (Darter et al., 2006) and LCFs for flexible pavement distress prediction used by the three states. Note that there are several other

calibration coefficients used by the distress prediction models; GCF values have been established for all the coefficients. However, Table 2.2 only shows the GCFs corresponding to the coefficients which have been calibrated to establish the corresponding LCFs. The LCF values were obtained from research reports published by the respective agencies based on their respective local calibration efforts (Mallela et al., 2013; Haider et al., 2014; Bayomy et al., 2018).

Table 2.2 Global and Local Calibration Factors used for Flexible Pavement Distress Prediction in the States of Idaho, Colorado, and Michigan

Performance Model	Calibration Coefficient	GCFs	LCFs		
			Idaho, ID	Colorado, CO	Michigan, MI
AC Rutting	$\beta 1_r$	1	3	1.34	0.9453
	$\beta 2_r$	1	1*	1*	1.3
	$\beta 3_r$	1	0.661	1*	0.7
Unbound Base Rutting	β_{s1}	1	0.53	0.4	0.0985
Subgrade Rutting	β_{s1}	1	0.477	0.84	0.0367
Bottom-up Fatigue Cracking	C1	1	1*	0.07	0.5
	C2	1	0.824	2.35	0.56
Top-Down Fatigue Cracking	C1	7	4.533	7*	2.97
	C2	3.5	0.229	3.5*	1.2
Fatigue damage model (AC fatigue)	β_{f1}	1	1*	130.3674	1*
	β_{f2}	1	1*	1*	1*
	β_{f3}	1	1*	1.217799	1*
Thermal Cracking	K1	1.5	2.169	7.5	0.75
	K2	0.5	0.835	0.5	0.5
	K3	1.5	2.169	1.5	4
IRI	C1	40	35*	35*	50.372
	C2	0.4	0.35	0.3	0.4102
	C3	0.008	0.008	0.02	0.0066
	C4	0.015	0.01	0.019	0.0068

Note: * same as GCF

As the current research effort is primarily focused on the effects of temperature change on flexible pavement performance, greater emphasis was given to flexible pavement distress types that have been known to be significantly affected by temperature. Accordingly, the distress types primarily considered in this study were: AC rutting and

thermal cracking. The following sections present brief descriptions of the AC rutting and thermal cracking prediction models incorporated into PMED.

AC rutting model

Rutting can be defined as the permanent deformation of the flexible pavement layers along the wheel path (Huang, Y. H., 2004, p. 35). Rutting can occur due to the plastic deformation of the AC layer(s), unbound aggregate layer(s), or the subgrade (Huang, Y. H., 2004, pp. 24, 374). The mechanistic analysis approach incorporated into PMED divides each layer of a pavement section into multiple sublayers. Subsequently, rut depths are computed at the mid-depth of each sublayer; these individual sublayer rut depths are finally summed to calculate the total pavement rutting. Equation 2.1 presents the transfer function used in PMED to predict AC rutting in a flexible pavement structure.

$$\Delta p_{(AC)} = \beta_{1r} k_z \varepsilon_{r(AC)} 10^{k_{1r}} n^{k_{2r}\beta_{2r}} T^{k_{3r}\beta_{3r}} h_{AC} \quad (2.1)$$

Where,

$\Delta p_{(AC)}$ = Accumulated permanent or plastic vertical deformation in the AC layer/sublayer, in.

$\varepsilon_{r(AC)}$ = Resilient or elastic strain calculated by the structural response model at the mid-depth of each AC sublayer, in./in.

h_{AC} = Thickness of the AC layer/sublayer, in.

n = Number of axle-load repetitions.

T = Mix or pavement temperature, °F

k_z = Depth confinement factor

$k_{1r,2r,3r}$ = Global field calibration parameters (k_{1r}= –3.35412, k_{2r}= 1.5606, k_{3r}= 0.4791)

$\beta_{1r}, \beta_{2r}, \beta_{3r}$ = Local or mixture field calibration constants.

From Equation 2.1 it can be seen that the β_{1r} coefficient corresponds to the resilient or elastic strain (ε_r) within the AC layer, whereas, β_{3r} is the exponent of the temperature variable (T). Given that the k values are the global coefficients and have constant values, it is evident that the temperature effect on AC rutting is primarily governed by the β_{3r} coefficient. Of course, it should be acknowledged that other parameters such as β_{1r} will be indirectly affected by temperature changes. This is because, change in temperature will affect the AC modulus, which in turn will affect the resilient strain magnitude under loading. Nevertheless, as evident from Equation 2.1, β_{3r} is the only parameter that is directly linked to the temperature value.

AC Thermal Cracking Model

Thermal cracking is another flexible pavement distress that is largely affected by temperature change. Asphalt is a temperature-dependent material, and its stiffness can vary over a wide range depending on temperature. At low temperatures, asphalt behaves as a stiff solid, and gradually turns into a viscous liquid with increasing temperature. Due to increased stiffness at low temperatures, AC layers in cold regions are more susceptible to thermal cracking than those in warmer areas. Equation 2.2 shows the transfer function corresponding to the PMED thermal cracking model.

$$TC = \beta_{t1} \mathrm{N} \left[\frac{1}{\sigma_d} log \left(\frac{C_d}{H_{HMA}} \right) \right] \quad (2.2)$$

Where,

TC = Observed amount of thermal cracking, ft./mi

β_{t1} = Regression coefficient determined through global calibration (400)

$N_{[z]}$ = Standard normal distribution evaluated at [z]

σ_d = Standard deviation of the log of the depth of cracks in the pavement (0.769), in.

C_d = Crack depth, in.

H_{AC} = Thickness of AC layers, in.

From the equation it can be observed that for a higher crack depth, the thermal cracking of the AC layer would be higher. Again, the crack propagation can be estimated using the Equation 2.3

$$\Delta C = A(\Delta K)^n \quad (2.3)$$

Where,

ΔC = Change in the crack depth due to a cooling cycle,

ΔK = Change in the stress intensity factor due to a cooling cycle, and

A, *n* = Fracture parameters for the AC mixture.

The stress intensity factor can be calculated using Equation 2.4

$$\mathrm{K} = \sigma_{\mathrm{tip}}[0.45 + 1.99\ (\mathrm{C_0})0.56] \quad (2.4)$$

Where,

σ_{tip} = Far-field stress from pavement response model at a depth of crack tip, psi

C_o = Current crack length, ft.

The fracture parameters A and n (in Equation 2.3) can be calculated using Equation 2.5 and Equation 2.6. With increasing magnitude of the fracture parameters (A and/or n), the crack depth (C_d) will also increase, which will eventually increase the thermal cracking (TC) of the AC layer. As seen from Equation 2.5, the fracture parameter 'A' is dependent on two important materials properties of the AC layer: (1) AC tensile

strength (σ_m); and (2) AC indirect tensile modulus (E_{AC}). Changes in either of these parameters can greatly affect the thermal cracking susceptibility of the AC layer.

$$A = k_t \beta_t 10^{[4.389 - 2.52 log(E_{HMA} \sigma_m n)]} \quad (2.5)$$

$$n = 0.8 \left[1 + \frac{1}{m}\right] \quad (2.6)$$

Where,

k_t = Coefficient determined through global calibration for each input level (Level 1 = 1.5; Level 2 = 0.5; and Level 3 = 1.5)

β_t = Local or mixture calibration coefficient

E_{AC} = AC indirect tensile modulus, psi

σ_m = Mixture tensile strength, psi

m = Derived from the indirect tensile creep compliance curve measured in the laboratory

The β_t factor in Equation 2.5 is the field calibration coefficient, which should be established through a state or local transportation agency's local calibration effort. However, the PMED software does not allow changing the β_t coefficient. Therefore, during the Idaho local calibration efforts, instead of "β_t," the global factors "K" were altered to accommodate local conditions during thermal cracking prediction (Bayomy et al., 2018). A similar approach was undertaken during Colorado and Michigan local calibration efforts (Mallela et al., 2013; Haider et al., 2014).

The AC tensile strength (σ_m) is a fundamental parameter in PMED low pavement temperature thermal cracking predictions. An asphalt mixture with high tensile strength would provide better thermal cracking performance. In contrast, if the tensile strength of

the mixture decreases, the AC layer will be more prone to thermal cracking. While accounting for temperature effects on material behavior, PMED assumes that with increasing temperature, the asphalt mixture tensile strength decreases, which eventually reduces the AC layer resistance to the cracking, thus making it more susceptible to thermal cracking. Besides, pavement cooling rate also affects the thermal cracking of the AC layer, which will be discussed in Chapter 3 of this thesis. Therefore, during pavement analysis and performance prediction using PMED, the AC thermal cracking depends on multiple factors such as pavement temperature, mix tensile strength, pavement cooling rate, etc. This understanding will be important during interpretation of the analysis results presented in Chapter 3 of this master's thesis.

CHAPTER THREE: RESEARCH METHODOLOGY AND FINDINGS

As stated in the earlier chapters, the initial goal of this study was to evaluate how the transfer functions inherent to PMED accommodate the effects of temperature changes during pavement analysis and performance prediction. This was accomplished by using a manual shifting approach to generate synthetic temperature distribution data. Once a good understanding of the PMED distress prediction mechanism was achieved, a more realistic approach was adopted to generate future temperature distributions using established GCMs. This chapter presents details regarding the specific data processing methods to generate temperature distributions representative of future climatic conditions, as well as findings from the PMED simulations run using different temperature distributions.

Data Processing Methods

This section provides a brief description of how the climatic data were generated in this study for analysis with PMED. Historical climatic data starting from 1985 for the nearest climate station of the location under consideration (Boise, Denver, or Detroit) were downloaded from the *M*odern-*E*ra *R*etrospective *A*nalysis for *R*esearch and *A*pplications (MERRA) database developed by the National Aeronautics and Space Administration (NASA) (NASA, 2009; Federal Highway Administration [FHWA] MERRA Climate Data for MEPDG Inputs, n.d.). The MERRA climatic data file consists of hourly distributions of Temperature (°F), Precipitation (in.), Wind Speed (mph), Percent Sunshine (%), and Relative Humidity (%), among others.

Two independent scenarios were considered during statistical manipulation of the temperature distribution: (1) Alter the mean (μ), and (2) alter the standard deviation (σ) of the temperature distribution. Researchers have projected that by 2100, the temperature of the Pacific Northwest would rise approximately by 3ºF and 10ºF (United States Environmental Protection Agency [EPA], n.d.). The scenarios initially considered to study the effects of temperature change on flexible pavement performance involved: (a) increasing the mean of the temperature distribution by 1°C (1.8°F), and (b) increasing the standard deviation of the temperature distribution by 10%. Later on, a third scenario, i.e. (c) increasing the mean of the temperature distribution by 5°C (9°F), was added to study the effect of extreme shifts in temperature distribution on flexible pavement performance.

Climatic data from four randomly selected Global Climate Models (GCMs) were also collected, and the temperature data was downscaled to facilitate its use with PMED. A period of twenty years between 2046-2065 was considered while working with the GCM-projected temperature data. This specific time frame was considered as the current study intended to study the effect of temperature change at a period that is about 30 years ahead, representing the middle of the 21st century. According to Pachauri et al. (2014), the global mean surface temperature change in the mid-21st century (2046-2065) could be up to 1°C to 2°C depending on the emission scenarios. Therefore, selection of this analysis time frame is in line with the temperature increase scenarios considered during the manual shifting process.

Generating Manually Shifted Temperature Distribution

Historical Climate Data

Before going into further details about data manipulation methods used to generate future temperature distributions, this section provides a brief description of the historical climatic data. The projected temperature patterns were synthetically generated through modification of the MERRA historical temperature data as well as downscaled GCM-projected temperature data. The FHWA LTPP InfoPave component known as "MERRA climate data for MEPDG inputs" has climatic data available from 1985 to 2018 for all the climate stations considered in this study, except for Boise, which has available data until mid of 2017 (FHWA MERRA Climate Data for MEPDG Inputs, n.d.).

Figure 3.1 compares the temperature distributions for Boise, Idaho (BOI) corresponding to the first (1985), and the last (2017) years, at different time scales ranging from a particular day to a month within the year.

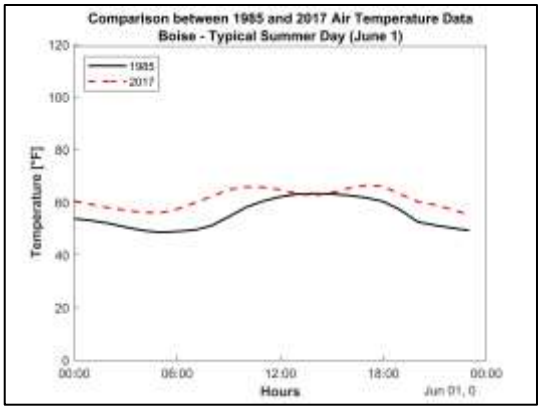

(a)

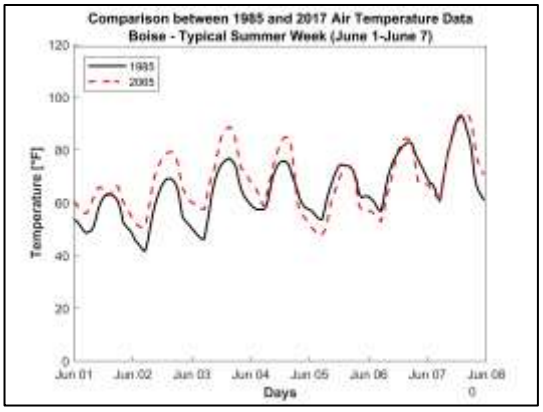

(b)

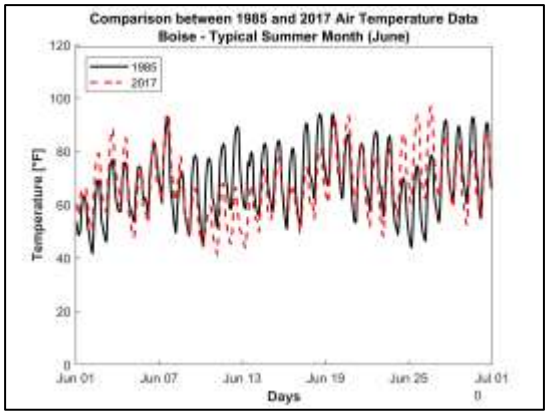

(c)

Figure 3.1 Comparison of 1985 and 2017 Temperature Data (a) Typical Day: Jan 01, 1985 & 2017; (b) Typical Week: Jan 01-07, 1985 & 2017; (c) Typical Month: Jan,1985 & 2017

Although the overall temperature distributions for the two years look similar, the individual values were significantly different from each other. The figures clearly show the wide range of temperatures experienced in Boise during a particular year.

Figure 3.2 compares the frequency distribution of full-year (Jan-Dec) historical temperature data for the years 1985 and 2017. Figure 3.2 indicates that the overall distribution shape for temperature data is similar for the two years considered. However, the temperatures in 2017 were greater than those in 1985. A similar trend was observed

for other cities (Denver and Detroit) considered in the study, but have been excluded from graphical representation in this thesis document for the sake of brevity.

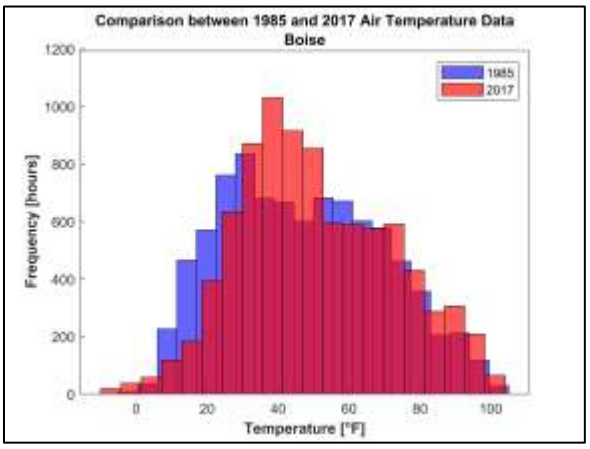

Figure 3.2 Comparing the Frequency Distribution of Full-Year Historical Temperature Data for Boise (1985 and 2017)

Full-Year Modified Temperature Data

This study used MATLAB® (Version 2019b; Mathworks, 2019) to develop a code that can modify the historical temperature data and create the manually shifted future/projected temperature distribution. The first task involved extracting the temperature data from the historical '.hcd' files, and determining what statistical distribution could be used to best describe the temperature patterns. From the analysis, it was determined that the Generalized Extreme Value (GEV) distribution worked best for the historical temperature data. The GEV distribution has three parameters: (1) Shape (ξ); (2) location (μ); and scale (σ) describing the nature of the distribution. Equation 3.1 taken from Wikipedia ("Generalized extreme value distribution," n.d.), shows the cumulative distribution function (CDF) and the probability density function of the GEV distribution.

$$F(x;\mu,\sigma,k) = exp\left\{-\left[1+\xi\left(\frac{x-\mu}{\sigma}\right)\right]^{-1/\xi}\right\} \quad (3.1)$$

Where,

ξ = Shape parameter

μ = location parameter

σ = scale parameter

This study primarily focused on the location and scale parameters, which represent mean and standard deviation of the distribution, respectively. Figure 3.3, obtained from Wikipedia ("Generalized extreme value distribution," n.d.), shows a typical shape of the GEV distribution corresponding to different shape parameter values.

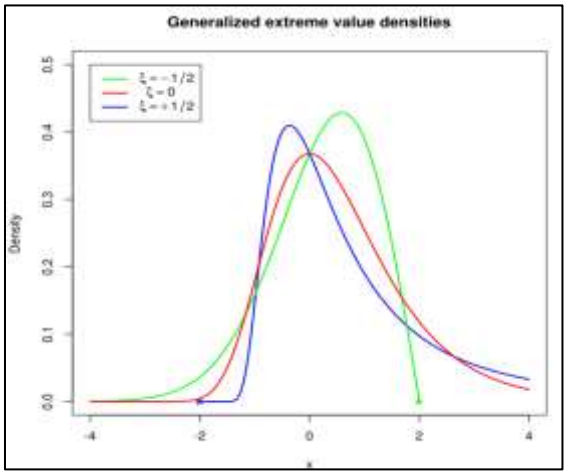

Figure 3.3 Graph Showing Shape of the Generalized Extreme Value (GEV) Distribution Corresponding to Different Shape Parameters

Once the GEV distribution was fit to the data, the mean (μ) and standard deviation (σ) values were determined, and corresponding Cumulative Distribution Functions (CDFs) were identified. The mean of the historical data was increased by 1.8ºF (1ºC) (σ remaining unchanged), and a probability distribution object was created using the shifted mean. The new temperature distribution was generated using the shifted

probability distribution object and the previously established CDF. Finally, the temperature values in the historical ".hcd" file were replaced by the newly generated (shifted) temperature values. All other climate parameters (precipitation, relative humidity, percent sunshine, wind speed, etc.) remained unchanged in the shifted database.

Figure 3.4 shows the frequency distribution of the temperature data for the three cities, e.g., Boise, Idaho (BOI); Denver, Colorado (DEN); and Detroit, Michigan (DTM), considered in this study before and after manual shifting by different values. Figure 3.4 (a) shows the historical temperature distribution, whereas Figures 3.4(b) and 3.4(c) show the temperature distribution after the mean (μ) was shifted by 1.8ºF (1º C) and 9ºF (5º C), respectively. A comparison between Figure 3.4(a) and Figure 3.4(b) clearly shows that shifting the mean by 1.8ºF results in an increase in the number of high-temperature days in all the studied locations.

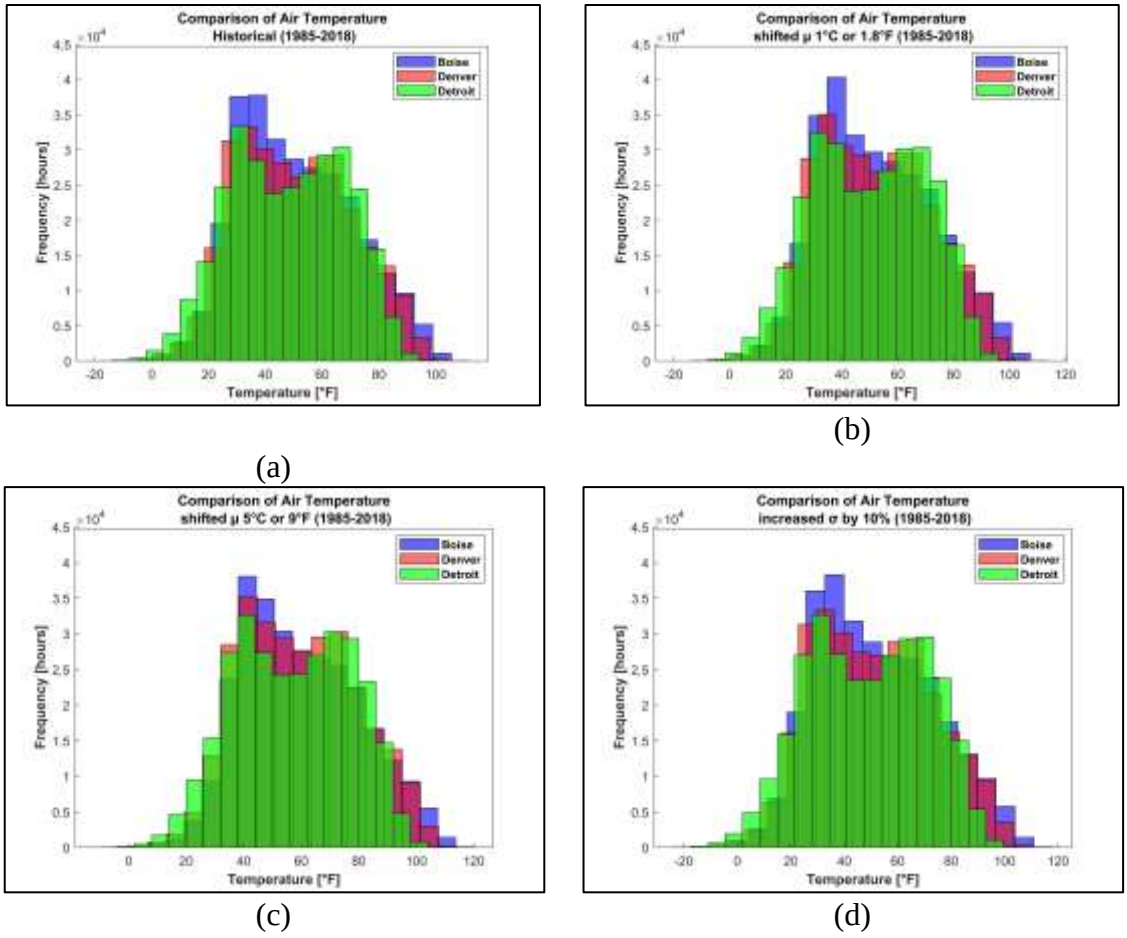

Figure 3.4 Frequency Distribution of the Temperature Distribution for Three Cities Considered in this Study: (a) Historical Case; (b) Increased μ by 1°C (1.8°F); (c) Increased μ by 5°C (9°F); (d) Increased σ by 10%

A similar trend can be observed by comparing Figures 3.4(a) and 3.4(c). Following the same data manipulation procedure, the other scenario of changed temperature distribution was simulated by increasing the standard deviation of the historical temperature distribution by 10%, while keeping the mean of the distribution unchanged (see Figure 3.4(d)). Note that an increase in standard deviation can be perceived as a widening of the distribution curve, with the location (mean) of the distribution curve remaining unchanged.

Table 3.1 lists the mean and standard deviation values for the historical and manually altered temperature distribution scenarios.

Table 3.1 Summary of the Mean and Standard Deviation Values for the Temperature Distributions Corresponding to the Different Scenarios

City	Historical		Shifted μ 1°C		Shifted μ 5°C		Increased σ by 10%	
	μ (°F)	σ (°F)	μ (°F)	σ (°F)	μ (°F)	σ (°F)	μ (°F)	σ (°F)
BOI	42.89	18.49	44.69	18.49	51.89	18.49	42.89	20.78
DEN	42.88	19.31	44.68	19.31	51.88	19.31	42.88	21.24
DTM	41.61	20.31	43.41	20.31	50.61	20.31	41.61	22.34

A comparison of mean temperature data indicates that the three cities selected for consideration in the current study have similar temperature conditions. With the temperature distributions being more-or-less similar, the effects of the LCFs on pavement performance predicted using PMED can be effectively isolated as discussed later in this chapter.

Seasonal Modification of Temperature Distributions

The above section represented a situation where the temperature distribution corresponding to the entire year was manipulated to generate the distributions corresponding to different scenarios. A second approach considered in this study was manually altering the statistical parameters for the temperature distribution corresponding to specific seasons (rather than the entire year). This was done to simulate situations where climate change is manifested in a manner so that summers become hotter, or winters become hotter, etc. This is particularly important while studying the temperature-dependent behaviour of AC layers in a flexible pavement system. For example, the rutting problem in flexible pavement becomes more significant when the temperatures become hotter. On the other hand, thermal cracking (also known as low-temperature cracking) becomes worse under extremely cold winters. Altering the seasonal

temperature distribution parameters, will therefore, facilitate investigation of the effects of such scenarios on pavement performance predictions. A standard hypothesis would be that rutting would increase when the summer gets hotter, and thermal cracking (at cold locations) would decrease when winters get warmer.

A simplistic approach was adopted to define the seasons of the year **(**see Table 3.2) in this study. Historical temperature data for each of the seasons was extracted, and a data manipulation procedure, identical to the one described above for the full-year distribution was followed to simulate the altered mean and standard deviation scenarios.

Table 3.2 Season Definitions used in the Current Study

Season	**Month**
Winter	December, January, February
Spring	March, April, May
Summer	June, July, August
Fall	September, October, November

Typical Pavement Section Design

A typical rural primary arterial pavement section was considered for analysis and performance prediction in this study. Historical climatic data for Boise, Idaho was used as the base case for the PMED simulations. The pavement section was first analyzed using PMED with the default Global Calibration Factors (GCFs). As already explained, the GCFs do not account for local conditions and use generic coefficient values to predict pavement performance based on the critical pavement response parameters. Over the years, several state highway agencies in the US have undertaken research/implementation studies to develop Local Calibration Factors (LCFs) that can be used for pavement

analysis and performance prediction in the corresponding states. All three states considered in the current study (Idaho, Colorado, and Michigan) have undertaken such calibration efforts (Mallela et al., 2013; Haider et al., 2014; Bayomy et al., 2018). Pavement analysis and performance prediction using PMED requires four generic types of input data: (1) General and reliability inputs; (2) Traffic; (3) Climate; and (4) Structural input with material characteristics.

Table 3.3 presents a summary of the preliminary design inputs considered during the first part of this study. The design inputs were collected from a database developed by the Idaho Transportation Department (ITD) as a part of their PMED implementation efforts (Bayomy et al., 2012; Mallela et al., 2014, Bayomy et al., 2018). The Hot-Mix Asphalt (HMA) binder type was selected using the LTPPBind Online tool (FHWA LTPPBind online, n.d.) based on MERRA historical climatic data for Boise. Based on the climatic data, it was found that at 98% reliability, the average seven-day maximum pavement temperature is 62.45 °C, and the minimum pavement temperature is -26.40 °C. Therefore, the Superpave performance grade PG 64-28 asphalt binder was selected for designing the pavement section. All the design inputs were kept unchanged between different simulations except for the temperature data in the climatic data files.

Table 3.3 Design Inputs used for the Design of a Representative Flexible Pavement Section Used in the Current Study

Design Parameter		**Input**
Pavement Section Design		State Highway
Performance Criteria & Reliability		Rural-Primary Arterials (reliability: 85% for all the distress types and IRI)
AADTT (Annual Avg. Truck Traffic		720
Growth Rate		3%
Vehicle Class Distribution		WIM 156 (SH 33)
Speed Limit		55 mph
Vehicle Axle Load Distribution		WIM 156 (Moderately Loaded)
Climatic Data		Boise Station (Lat. 43.5; long. -116.25)
Pavement Structure	AC	6 in.; PG 64-28
	Base	6 in.; Mr: 40,000 psi (A-1-a)
	Subbase	12 in.; Mr: 30,000 psi (A-2-4)
	Subgrade	Semi-infinite; Mr: 9000 psi (A-2-7)

Analysis of Temperature Sensitivity of PMED Distress Predictions: Manually Shifted Results

PMED uses distress prediction models to translate the critical pavement response parameters obtained from the mechanistic analyses into distress development in the pavement structure throughout its service life. The following flexible pavement distresses are used to determine the adequacy of a particular design alternative: Total Pavement Rutting, AC Rutting, Bottom-Up Fatigue Cracking, Top-Down Fatigue Cracking, AC Thermal Cracking or Transverse Cracking, and International Roughness Index (IRI).

Threshold values corresponding to each of these distress types were obtained from ITD's design manual (Mallela et al., 2014); threshold values used for total pavement rutting, AC rutting, AC thermal cracking, and AC bottom-up fatigue cracking were 0.5 in., 0.5 in., 1500 ft./mile, and 15.00 % lane area, respectively (Mallela et al., 2014). The PMED-predicted distresses under different climatic scenarios were compared to assess the sensitivity of the pavement performance prediction approach to the temperature changes. Three distress types that are most likely to be affected by temperature changes (pavement rutting, thermal-cracking) have been discussed in this thesis document for the sake of brevity. AC top-down fatigue cracking prediction was not included in the analysis because the PMED manual of practice does not recommend using the current top-down cracking model for design purposes. The current version (2.5.5) of PMED has not been calibrated with the recently developed top-down cracking models (Lytton et al., 2018). Moreover, IRI was excluded from the analysis because the IRI prediction depends on all the other distress types, and some other factors (such as a site factor), which is not directly related to temperature change.

Comparison between Historical and Manually Altered Temperature Distributions: Boise

Tables 3.4 and 3.5 summarize the results from PMED simulations corresponding to the cases where the historical and manually shifted temperature distributions for Boise were used as input. Results corresponding to the GCFs have been tabulated in Table 3.4, whereas Table 3.5 lists the results corresponding to Idaho-established LCFs.

Table 3.4 Summary of Predicted Pavement Distresses for Boise Climatic Data and Global Calibration Factors

Climatic Condition	Data type	Distress Predicted		
		Total Pavement Rutting (in.)	AC Rutting (in.)	AC Thermal Cracking (ft./mile)
Historical	Entire Year	0.43	0.11	270.98
Shifted mean (μ) 1°C	Entire Year	0.44	0.12	733.99
	Winter	0.43	0.11	587.67
	Spring	0.43	0.11	781.15
	Summer	0.44	0.12	781.15
	Fall	0.43	0.11	777.52
Incr. SD (σ)	Entire Year	0.45	0.13	2399.10
	Winter	0.43	0.11	1975.87
	Spring	0.43	0.11	769.06
	Summer	0.44	0.12	767.86
	Fall	0.43	0.12	772.69

Table 3.5 Summary of Predicted Pavement Distresses for Boise Climatic Data and Local Calibration Factors

Climatic Condition	Data type	Distress Predicted		
		Total Pavement Rutting (in.)	AC Rutting (in.)	AC thermal cracking (ft./mile)
Historical	Entire Year	0.37	0.13	721.90
Shifted mean (μ) 1°C	Entire Year	0.38	0.14	372.43
	Winter	0.37	0.13	378.48
	Spring	0.37	0.13	718.27
	Summer	0.38	0.14	717.06
	Fall	0.37	0.13	715.86
Incr. SD (σ)	Entire Year	0.39	0.15	2000.05
	Winter	0.37	0.13	1383.35
	Spring	0.37	0.13	723.10
	Summer	0.38	0.14	721.90
	Fall	0.37	0.13	724.32

From the simulation results it can be seen that the predicted distresses do not change significantly due to the increase in temperature. Simulation results exhibit little differences in total pavement rutting and AC rutting predictions between the historical and projected temperature cases. This is true for scenarios where the temperature distribution was altered for the entire year, as well as when the summer seasons were artificially made warmer.

Thermal cracking predictions showed considerable sensitivity to increase in mean and standard deviation of temperature distribution irrespective of whether the change was

implemented for the entire year's data or just for certain seasons. From Table 3.4 it can be seen that for all the projected cases, the predicted thermal cracking increased due to increase in temperature, with the highest cracking observed when the SD of full-year temperature data increased. On the other hand, results from Table 3.5 (corresponding to LCFs) show that the predicted thermal cracking magnitudes decrease for almost all the projected cases except when SD of the full year and winter temperature data increased. AC thermal cracking in flexible pavements is generally related to cold temperatures, and intuitively speaking, the thermal cracking magnitudes should be less under warmer climates. However, the PMED-predicted thermal cracking values do not follow this expected pattern. This is primarily because AC thermal cracking in flexible pavements depends on several other parameters beside the absolute temperature. Two such parameters are the cooling rate of pavement layer and indirect tensile strength of the AC layer. Apeagyei et al. (2008) studied the effect of cooling rate on the AC thermal cracking using the thermal cracking model (TCMODEL), which is also incorporated into PMED for thermal cracking predictions. From the analysis of TCMODEL predictions, they concluded that pavement cooling rate significantly affects the thermal cracking in flexible pavements. Moreover, it should be noted that the algorithms inherent to PMED assume that with the increase in temperature, the indirect tensile strength of asphalt concrete decreases. This, in turn, would make the AC layer more susceptible to thermal cracking even under warmer climates. Therefore, the predicted AC thermal cracking values do not follow the intuitive trend of reduced cracking under warmer climates.

For simulations using GCFs as well as LCFs, the AC bottom-up fatigue cracking at the end of the design period didn't change much due to the change in temperature.

Accordingly, discussions about bottom-up fatigue cracking have been eliminated from this thesis.

From the results presented in Tables 3.4 and 3.5, it appears that the effect of increasing the standard deviation of full-year temperature distribution has a greater impact on total pavement rutting and AC rutting compared to increasing the corresponding mean values. Finally, among the seasonal temperature cases, only an increase in summer temperature produced slightly higher pavement distresses for the considered pavement section of Boise.

Comparison between Historical and Manually Altered Projected Cases: Multiple Cities

As evident from the above discussion, temperature change was found to have minimal effects on pavement rutting predictions for the primary study location, i.e., Boise, ID. This was true for simulations with both GCFs as well as LCFs. This raised questions about the sensitivity of PMED in capturing the effect of increased temperatures while predicting flexible pavement performance. To further investigate this aspect, similar analyses were performed for two more cities: Denver (Colorado) and Detroit (Michigan). As previously mentioned, the temperature distributions for the three cities (Boise, Denver, and Detroit) were more or less similar to each other. Note that similarity between the distributions in the present context refers to the shape of the temperature distribution as well as the mean values. Therefore, PMED simulations with climatic conditions at these locations would give insight into two different aspects. Firstly, as the temperature distributions for the three cities are similar, PMED simulation results with GCFs should indicate similar sensitivity to temperature changes for the three locations. Secondly, PMED simulations with LCFs at these locations will clearly compare the effect

of LCFs used by the three states (Idaho, Colorado, and Michigan) in predicting pavement performance under varying climatic conditions. Besides the different temperature distribution scenarios discussed above, this section also compares pavement performance predictions at the three cities under an extreme condition where the mean of the historical temperature distribution is increased by 9°F (5°C). Note that all design inputs (except for the temperature data) were kept unchanged from the base case (for Boise) during this multi-location comparative effort. LCFs established by the corresponding states were used during the analyses.

Tables 3.6 and 3.7 present results from this multi-location comparative effort. Table 3.6 presents results corresponding to the GCFs, whereas results from simulations with LCFs have been listed in Table 3.7. As evident from Table 3.6, the change in rutting predictions with changing temperature was similar for all three locations. For example, the predicted AC rutting for Boise changed from 0.11 in. to 0.12 in. when the mean temperature was increased by 1°C. Similarly, the predicted AC rutting for Denver and Detroit changed from 0.24 in. to 0.25 in., and 0.08 in. to 0.09 in., respectively. Somewhat similar behavior was observed in the predicted AC rutting values when the mean temperature was increased by 5°C, and the standard deviation was increased by 10%. However, it should be noted that unlike the AC rutting predictions, the thermal cracking predictions did not follow similar patterns for the three locations. This may be attributed to the compounding factors governing AC thermal cracking behavior.

Table 3.6 Summary of Predicted Pavement Distresses for Multiple Cities Climatic Data and Global Calibration Factors

Climatic Condition	Total Pavement Rutting (in.)			AC Rutting (in.)			AC Thermal Cracking (ft./mile)		
	BOI	DEN	DTM	BOI	DEN	DTM	BOI	DEN	DTM
Historical	0.43	0.39	0.41	0.11	0.24	0.08	270.98	175.92	686.83
Shifted mean (μ) 1°C	0.44	0.40	0.42	0.12	0.25	0.09	733.99	175.17	590.09
Shifted mean (μ) 5°C	0.46	0.45	0.43	0.15	0.30	0.11	2169.34	356.50	356.50
Incr. SD (σ)	0.45	0.42	0.43	0.13	0.27	0.09	2399.10	228.41	2036.33

Table 3.7 Summary of Predicted Pavement Distresses for Multiple Cities Climatic Data and Local Calibration Factors

Climatic Condition	Total Pavement Rutting (in.)			AC Rutting (in)			AC Thermal Cracking (ft/mile)		
	BOI	DEN	DTM	BOI	DEN	DTM	BOI	DEN	DTM
Historical	0.37	0.75	0.32	0.13	0.42	0.29	721.90	2592.57	175.13
Shifted mean (μ) 1°C	0.38	0.78	0.34	0.14	0.45	0.32	372.43	2592.57	175.12
Shifted mean (μ) 5°C	0.41	0.89	0.43	0.17	0.56	0.41	356.56	1879.12	356.50
Incr. SD (σ)	0.39	0.81	0.36	0.15	0.48	0.34	2000.05	2592.57	177.89

From the summary of the simulation results (with LCFs) presented in Table 3.7, it can be observed that the AC rutting predictions for Boise show less sensitivity to temperature change compared to the two other locations. This is clearly evident from results corresponding to the extreme case where the mean historical temperature was shifted by 5°C (9°F). Even for such a drastic change, the predicted AC rutting for Boise

changed by only 0.04 in. (from 0.13 in. to 0.17 in.). On the other hand, the AC rutting prediction for Denver changed from 0.42 in. to 0.56 in., and that for Detroit changed from 0.29 in. to 0.41 in. This indicates that there are some differences between the LCFs used by the three states that lead to such drastically different sensitivities in AC rutting prediction with increasing temperature. This aspect was investigated as the next step in this thesis research. Note that the thermal cracking predictions listed in Table 3.7 did not show any consistent pattern between the three states. When the mean temperature was increased by 5°C, the AC thermal cracking for Boise and Denver decreased, whereas that for Detroit increased.

Temperature Sensitivity Analysis Using PMED Rutting Prediction Model

Rutting prediction results from the multi-location comparison presented in the above section highlighted the insensitivity of LCFs used in Idaho to temperature changes. A temperature sensitivity study was performed using the PMED rutting transfer function to investigate the effect of LCF values.

Table 3.8 lists the LCFs for AC rutting established by the three states being compared in the current study. These calibrations factors are used in the transfer function presented in Equation 2.1. From Table 3.8 it can be seen that the Beta *(β)* coefficient values vary widely from one state to another, especially the values of *β1* and *β3*. The K-coefficient values, on the other hand, are identical for the three states as they correspond to the GCFs. As shown in Equation 2.1, *β1* is the coefficient corresponding to the elastic strain (ε) in the asphalt layer, and *β3* factor is the exponent of the temperature (T) variable in the transfer function. Accordingly, *β3* directly affects how the transfer function captures the effect of temperature variations while predicting AC rutting.

Table 3.8 Comparison of Studied States LCFs Established for the AC Rutting Prediction Model

Prediction Model	Calibration Coefficient	LCFs		
		ID	CO	MI
AC Rutting	β1r	3	1.34	0.9453
	β2r	1	1	1.3
	β3r	0.661	1	0.7
	K1r	-3.35412	-3.35412	-3.35412
	K2r	1.5606	1.5606	1.5606
	K3r	0.4791	0.4791	0.4791

Table 3.9 lists how changing the *β3 and T* values (either simultaneously or separately) affects the AC rutting predictions. Using the AC rutting transfer function, considering all other variables of the transfer function to be constant, the AC rutting was calculated for three different scenarios based on different *β3* and T values. The first involved increasing *β3* values while the T was kept constant. As expected, it was found that as the *β3* increases, the calculated AC rutting also increases. Similarly, calculated rutting also increases when both *β3* and T increase (second scenario).

Table 3.9 Sensitivity Analysis of PMED AC Rutting Transfer Function

Analysis Scenario	β3	T	Calculated $\Delta P_{(HMA)}$
β3 increasing and T constant	0.4	50	0.19
	0.661	50	0.31
	0.8	50	0.41
	1	50	0.59
both β3 and T increasing	0.4	30	0.17
	0.661	50	0.31
	0.8	70	0.46
	1	80	0.74
β3 decreasing and T increasing	1	30	0.15
	0.8	50	0.27
	0.666	70	0.35
	0.4	80	0.28

However, when the *β3* values decrease, but the temperature increases (third scenario), the rutting predictions reduce significantly. In other words, this clearly establishes that if a low value of *β3* is established during local calibration efforts by a state highway agency, then the corresponding transfer function will be relatively insensitive to temperature variations while predicting AC rutting.

From the coefficients listed in Table 3.8 it can be clearly seen that Idaho has the highest *β1* value *(β1* = 3), but the lowest β3 value *(β3 = 0.661)* among the three states being compared. This indicates that based on the LCFs used in Idaho, AC rutting is primarily governed by elastic strain in the asphalt layer, whereas the effect of temperature

changes is minimal. This is the reason, the PMED simulations using Idaho LCFs were relatively insensitive to temperature variations. Even the relatively large value of $\beta 1$ for Idaho did not lead to a noticeable increase in AC rutting with increasing temperatures. From Table 3.8 it can also be seen that the $\beta 3$ value for Colorado was the highest ($\beta 3 = 1.0$), whereas that for Michigan ($\beta 3 = 0.7$) was greater than that for Idaho ($\beta 3 = 0.661$), but lower than that for Colorado ($\beta 3 = 1.0$). Based on this observation, it is expected that the PMED simulations for Colorado would show the highest temperature sensitivity as far as AC rutting is concerned. This can be easily verified by the results presented in Table 3.7.

Effect of LCFs on PMED Rutting Predictions Studied using different LCF and Climatic Data Combinations

PMED simulation results corresponding to manual shifting of temperature distributions and the sensitivity analysis of the AC rutting prediction transfer function revealed that the effect of temperature change does not have a similar impact on pavement distress predictions at the three different locations under consideration. For example, Boise was found to have very little sensitivity to temperature changes, whereas results for Denver showed the highest temperature sensitivity, particularly in terms of AC rutting. This section presents findings from further PMED simulations performed to isolate the effects of varying LCFs from those of varying climatic data. The primary objective of this exercise was to investigate the underlying reason behind the insensitivity of PMED simulation results for Idaho to temperature variations.

To accomplish this objective, nine (9) different combinations of LCF and climatic data were considered, and PMED simulations were run for each combination. The combination considered were:

1. Use the manually shifted climatic data for Boise with LCFs from the three different states (ID, CO, MI)
2. Use the manually shifted climatic data for Denver with LCFs from the three different states (ID, CO, MI)
3. Use the manually shifted climatic data for Detroit with LCFs from the three different states (ID, CO, MI)

The simulation for each scenario was performed in a way where the respective local calibration factors available for each studied state were considered as the only variable instead of considering the climatic data as the variable of the design. In other words, for each scenario, three different simulations were run using three states LCFs and one common city's climatic data where all the inputs were kept the same except the LCFs.

Table 3.10 summarizes the results from the considered simulation scenarios. From Table 3.10 it can be observed that for all three simulation scenarios, while using the Idaho LCFs, the predicted rutting values exhibited minimal change from the base (historical) case to the different projected climatic conditions. In contrast, simulation results corresponding to LCFs from the two other states, increased sensitivity to temperature variations were observed. The findings from those simulations further reinforced the hypothesis that the LCFs for Idaho were established in a manner that the AC rutting predictions were rendered relatively insensitive to temperature variations.

Table 3.10 Summary of Simulation Results obtained from Different LCFs Analysis Scenarios

Simulation Scenario	Total Pavement Rutting (in.)			AC Rutting (in)		
	State LCF					
	ID	CO	MI	ID	CO	MI
	Using Boise (BOI) Climatic data					
Historical	0.37	0.78	0.44	0.13	0.45	0.42
Shifted mean (μ) 1°C	0.38	0.80	0.47	0.14	0.47	0.45
Shifted mean (μ) 5°C	0.41	0.92	0.59	0.17	0.60	0.57
Incr. SD (σ)	0.39	0.84	0.52	0.15	0.52	0.49
	Using Denver (DEN) Climatic data					
Historical	0.36	0.75	0.41	0.12	0.42	0.38
Shifted mean (μ) 1°C	0.37	0.78	0.43	0.13	0.45	0.41
Shifted mean (μ) 5°C	0.39	0.89	0.54	0.15	0.56	0.52
Incr. SD (σ)	0.38	0.81	0.47	0.14	0.48	0.45
	Using Detroit (DTM) Climatic data					
Historical	0.34	0.68	0.32	0.09	0.33	0.29
Shifted mean (μ) 1°C	0.35	0.70	0.34	0.10	0.36	0.32
Shifted mean (μ) 5°C	0.37	0.79	0.43	0.13	0.46	0.41
Incr. SD (σ)	0.36	0.36	0.36	0.11	0.11	0.34

Impact of Air Temperature Change on Pavement Temperature and AC Layer Modulus

The above sections presented the argument that the LCFs used in the state of Idaho were established in a manner that rendered the AC rutting transfer function relatively insensitive to temperature variations. However, all the analyses presented above were based on changes in air temperature as the primary reference. It is well-

known that temperature-dependent behaviour of flexible pavements is governed by the pavement temperature and not the air temperature. Therefore, the next step in this research effort was to analyze the intermediate files generated during PMED simulations to investigate how the different temperature distributions representing future climatic conditions affected the pavement layer temperatures. Moreover, variations in the AC sublayer moduli were also studied. If the pavement layer temperatures, as well as the AC sublayer moduli are found to exhibit expected trends, then it would be clearly established that the only factors rendering Idaho simulation results insensitive to temperature variations, were the LCFs.

The distress models inherent to M-E pavement design do not directly use the air temperature to predict pavement response and performance. Instead, the Enhanced Integrated Climatic Model (EICM) (Larson & Dempsey, 1997) uses air temperature as an input and generates the mean, standard deviation, monthly quintile temperature (dividing the monthly temperature distribution into five equal groups), and hourly pavement temperature as outputs, which then directly feed into the different PMED distress prediction models. The monthly mean, standard deviation, and quintile points are used by the permanent deformation and fatigue prediction models, whereas the hourly pavement temperature data of the bound layers is used by the thermal cracking prediction model. Details of pavement EICM output data, as well as the layer modulus calculation process of each pavement sublayer and PMED performance prediction methodologies have been discussed in chapter 3 of the NCHRP 1-37A final report (ARA. 2004) and in chapter 5 of the MEPDG 3rd edition (AASHTO, 2020).

The current study evaluated the impact of the air temperature on pavement sublayer temperature as well as the AC sublayer modulus for two of the studied locations (Boise, and Denver). Note that the values for Detroit have been eliminated from this particular section for the sake of brevity. Also, as previously discussed, the PMED simulation results for Denver and Boise exhibited the highest and lowest temperature sensitivities, respectively. Therefore, close examination of the pavement temperature and AC sublayer modulus data for these two locations would provide the required information. It is expected that the values for Detroit would follow a similar pattern. The algorithms inherent to PMED assume the temperature data to be normally distributed and divides the data into five equal quintiles (each quintile comprising 20% of the data). The first quintile represents the lowest data points of the distribution, whereas the fifth quintile represents the highest data points. Note that the PMED intermediate files corresponding to only one of the simulation scenarios (where the mean temperature has been shifted by 5°C to represent extremely warm climates in the future) have been discussed here for the sake of brevity.

Figure 3.5 compares the monthly fifth (5^{th}) quintile temperature distributions for the historical and projected years for Boise and Denver. These temperature values were obtained from the respective PMED intermediate files named *'_fatigue.dat.'* This file records the monthly quintile pavement temperatures of each AC sublayer. It also reports the mean and standard deviation of each month's temperature data. Figures 3.5(a) and 3.5(b) show the comparison between historical and projected quintile pavement temperatures for the AC surface and AC-bottom layers, respectively, corresponding to the Boise climatic data. For both layers, higher 5^{th} quintile pavement temperatures were

observed for the future case compared to the historical case. This clearly establishes that the increased air temperatures generated in this study indeed results in increased pavement temperatures. A similar trend was observed for Denver as shown in Figures 3.5(c) and 3.5 (d).

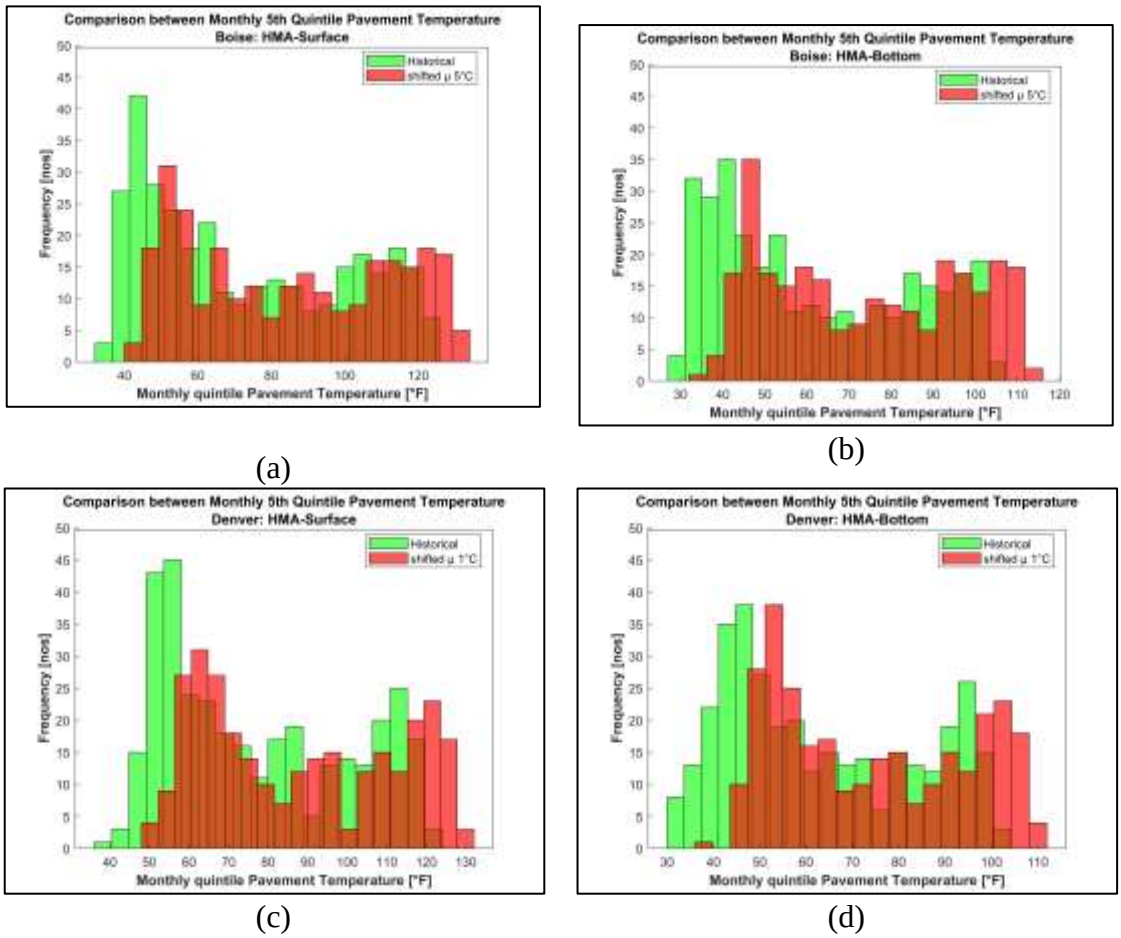

Figure 3.5 Comparison between the Monthly 5th Quintile Pavement Temperature of the Historical and Projected Case: (a) Boise - AC Surface; (b) Boise - AC Bottom; (c) Denver - AC Surface; (d) Denver - AC Bottom

Once it was established that the change in air temperature led to corresponding change in AC sublayer temperature, the next step was to investigate how these increased pavement temperatures affected the AC sublayer moduli. Generally, an increase in air temperature increases pavement temperature, and eventually, decreases the AC layer modulus. The *"layermodulus.tmp*" intermediate file, generated during PMED simulations

documents each AC sublayer modulus for each monthly quintile temperature. It also records the modulus values for the base, subbase, and subgrade layers at different depths. Figure 3.6 compares the AC sublayer modulus values between the historical and projected case at the surface and bottom of the AC layer, calculated for the 5^{th} quintile pavement temperature. Figures 3.6 (a) 3.6(b) compare the AC surface and bottom sublayer moduli, respectively, for the Boise climatic data. It can be observed that the distribution of the AC layer modulus calculated corresponding to the 5^{th} quintile temperature data is higher for the historical (base) case compared to the projected case. This is expected as increasing air temperature in the projected case would ultimately lead to reduced AC modulus. Similar data for Denver have been presented in Figures 3.6(c) and 3.6(d). It should be noted that a significant difference between the historical and projected AC sublayer moduli was observed for Denver, whereas the difference for Boise was not as significant.

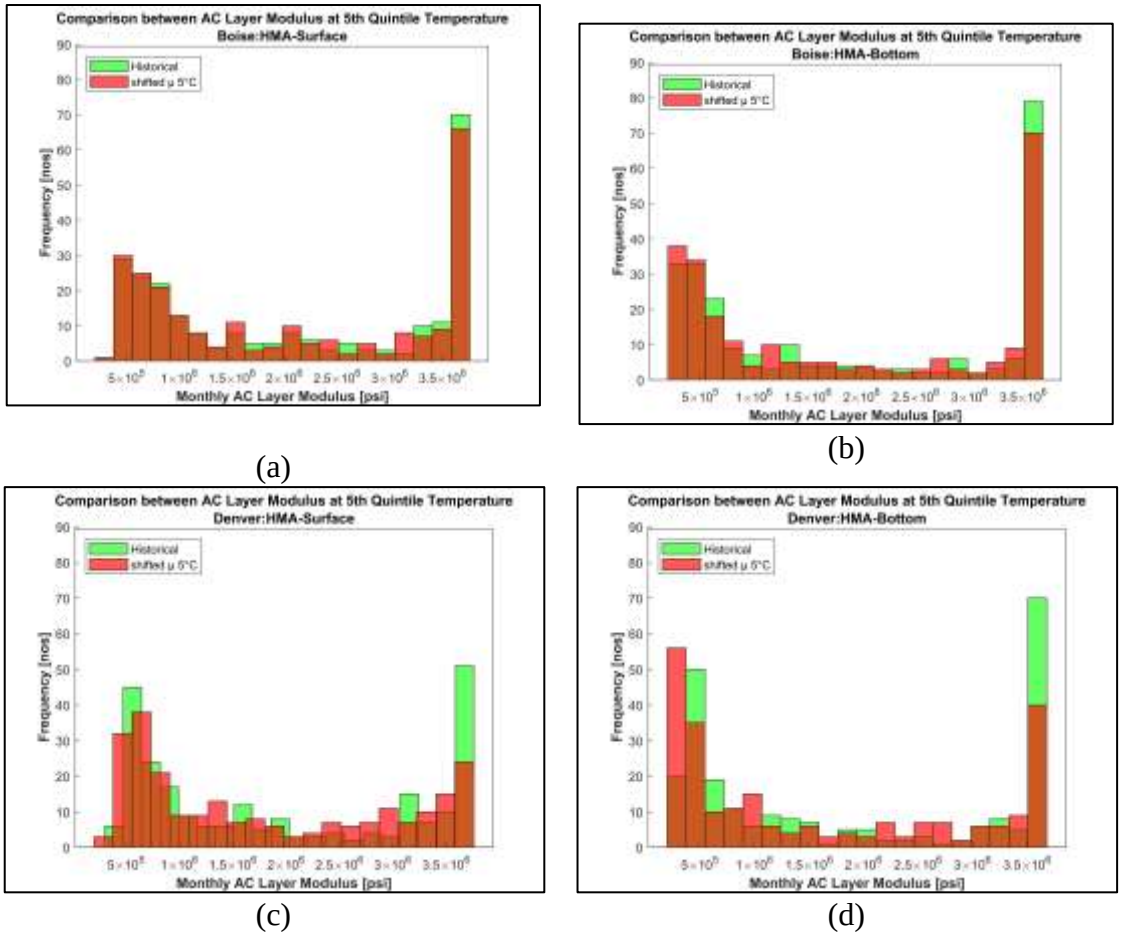

Figure 3.6 Comparison between the AC Sublayer Modulus of the Historical and Projected case: (a) Boise - AC Surface (b) Boise - AC Bottom; (c) Denver - AC Surface (b) Denver - AC Bottom

Another critical parameter to study from the intermediate data file was the hourly pavement temperature. The *'thermal.dat'* intermediate files documents the hourly pavement temperature profile with respect to depth of the AC layer. Figure 3.7 shows the comparison between AC surface and bottom hourly temperature distributions corresponding to the historical and projected climatic cases; data for both Boise and Denver have been presented

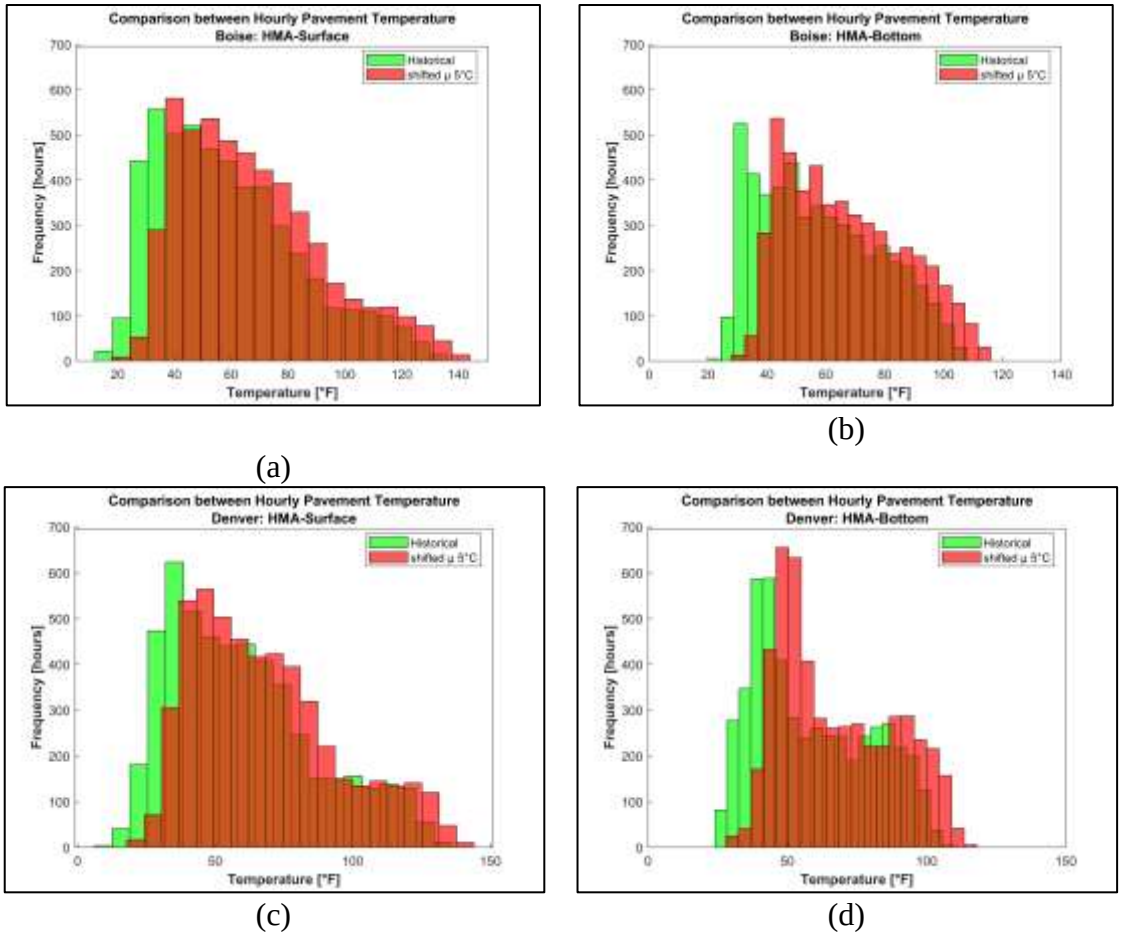

Figure 3.7 Comparison between the Hourly Pavement Temperature at the End of Historical and Projected Case: (a) Boise - AC Surface; (b) Boise - AC Bottom; (c) Denver - AC Surface; (d) Denver - AC Bottom

Figures 3.7(a) and 3.7(b) show that for Boise, the AC surface and bottom temperature changed significantly at the end of the pavement design life. This is expected as the projected air temperatures will be the highest at the end of the design period. Figures 3.7(c) and 3.7(d) present the same data for Denver, where the trends are identical to that for Boise.

Overall, the results presented in this section confirmed that air temperature change has a significant impact on the pavement quintile temperatures, AC sublayer moduli, as well as hourly pavement temperature distributions within the AC layer. Findings from that parametric analysis established that PMED was able to adequately transfer the

increased air temperatures into increased pavement temperatures using the EICM. Accordingly, the relative insensitivity of Idaho simulation results to temperature increase is most likely due to the nature of the established LCF values. Before making a final conclusion regarding this, the final task was to investigate the temperature sensitivity of the dynamic modulus data for the asphalt mix used in the pavement section. This was done to eliminate the possibility that the base (historical) temperature for Boise lies in a "flat" region of the dynamic modulus curve, leading to insignificant change in AC modulus even when the temperature is increased by 5°C. Results from this investigation are presented in the following section.

Impact of Air Temperature Change on Dynamic Modulus (E*) of Asphalt Mix

As already mentioned, this task aimed at studying the change in dynamic modulus of the asphalt mix used in the pavement section when the temperature values were changed. The dynamic modulus data for the asphalt was obtained from a database established for ITD by Bayomy et al. (2018). The primary objective was to plot the dynamic modulus (E*) master curve for the particular asphalt mix against temperature. The E* value corresponding to the mean AC surface temperature from the historical temperature distribution was identified. Then this value was "shifted" by 5º C and the corresponding E* values were read for two different frequencies (0.1 Hz and 10 Hz). This exercise would give an idea about the temperature sensitivity of the E* data for the particular mix.

Figure 3.8 shows the results from this exercise. For example, considering the E* vs. temperature curve corresponding to 0.1 Hz, the mean AC surface temperature of 59 °F corresponding to the base condition yields an E* value of 445090 psi. However, when

the temperature is shifted by 5ºC (or 9°F), the E* value reduces to 239528 psi. As the mean AC surface temperature increases by 5°C, the AC dynamic modulus decreases by 205562 psi. Similarly, for the modulus vs. temperature curve corresponding to 10 Hz, increasing the mean AC temperature by 5°C leads to a reduction in AC dynamic modulus by 350598 psi (from 1215832 psi to 865234 psi). Therefore, it can be summarized that the AC dynamic modulus (E*) of the mix used in this study shows significant temperature sensitivity. This temperature sensitivity should ultimately be reflected in the pavement performance predictions.

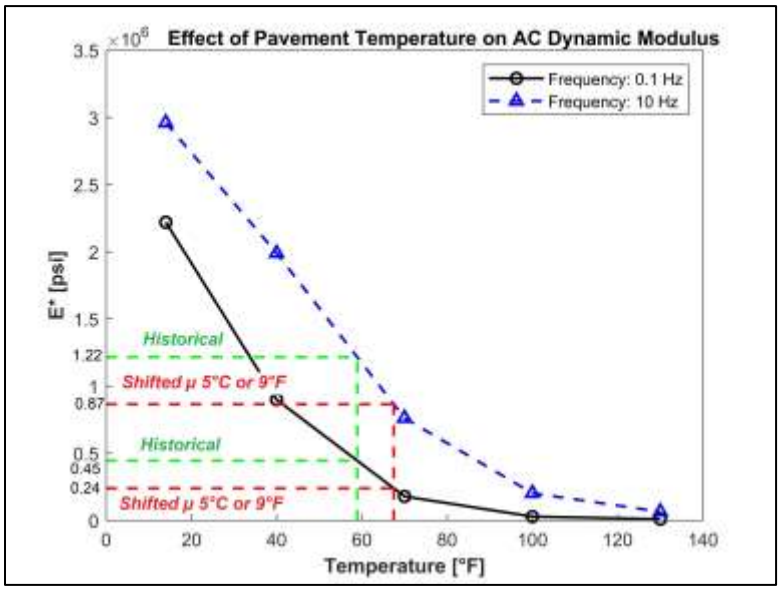

Figure 3.8 Effect of Temperature Change on Dynamic Modulus (E*) of Asphalt Binder (PG 64-28)

Using Generalized Climatic Models (GCMs) to Project Temperature Data

The first part of the current research study focused on artificially shifting the historical temperature distribution to generate synthetic temperature distributions for the future. This temperature data was then used as input during PMED simulations to study the effect of varying temperatures on flexible pavement performance prediction. The

primary focus during the first part was to get an in-depth understanding of the PMED transfer functions, and how the temperature changes were captured by the transfer functions during pavement analysis and performance prediction. Once that objective was accomplished, the next task involved generating more realistic temperature distributions for the future using Global Climatic Models (GCMs). Twenty (20) GCMs of the *C*oupled *M*odel *I*nter-Comparison *P*roject-Phase 5 (CMIP5) (Taylor et. al., 2012) were collected from the *M*ultivariate *A*daptive *C*onstructed *A*nalogs (MACA) dataset (Abatzoglou & Brown, 2012). The MACA is a statistical downscaling procedure to downscale the GCMs. Further details on MACA statistical procedures can be obtained elsewhere (Abatzoglou & Brown, 2012). . Future climatic data for approximately 100 years (2005-2100) were projected based on two different *R*epresentative *C*oncentration *P*athway (RCP) scenarios, e.g., RCP 4.5 and RCP 8.5.

A total of four (4) different types of pathway scenarios (RCP 2.6, RCP 4.5, RCP 6, and RCP 8.5) are available depending on the level of future green-house CO_2 emission. In other words, RCP scenarios mainly depend on the mitigation measures that will be considered to prevent the effect of future climate change. For example, RCP 2.6 means stringent mitigation measures will be taken to avoid the impact of climate change, which eventually stops the CO_2 emission in the mid of the 21st century. However, RCP 8.5 is an extreme scenario that considers no mitigation measures will be taken, and the CO_2 emission will continue in the 21st century and beyond (Pachauri et al., 2014). The RCP 4.5 and RCP 6 are intermediate scenarios considering that some mitigation steps will be adopted in the future to lessen the CO_2 emission and climate change effects. The range of global mean surface temperature change in mid- (2046-2065) and late- (2081-2100) 21st

century was predicted based on the different RCP scenarios. Pachauri et al. (2014) presented detailed information about the different RCP scenarios; detailed discussions on the different scenarios are beyond the scope of the current master's thesis. Note that both RCP 4.5 and RCP 8.5 scenarios were considered to project future temperature distribution data, that were subsequently used during PMED simulations.

Downscaling of Daily GCM-Projected Temperature Data to Hourly Data

All parameters in the GCM-projected climatic dataset are similar to those in the MERRA historical climatic database except for the percent sunshine (%). GCM dataset consists of solar radiation (%) instead of percent of sunshine (%). However, this is not significant in the present context as the primary focus of the current thesis research was to study the effect of temperature changes on flexible pavement performance. Even for cases where the future temperature was projected using the GCMs, all other climatic parameters were kept the same as the MERRA historical dataset.

The first task before using GCM-projected temperature distributions with PMED was to downscale the data. The PMED software and the inherent *E*nhanced *I*ntegrated *C*limatic *M*odel (EICM) require hourly climatic data as inputs. However, the GCM-projected datasets consist of daily data for all climatic parameters, including daily maximum and daily minimum temperatures. Accordingly, the first step in this work involved downscaling of the temperature data from a "daily scale" to an "hourly scale". This was accomplished by using the "Modified Imposed Offset Morphing Method (M-IOMM)" developed by Belcher et al. (2005). This specific method was taken from a similar study conducted by Gudipudi et al. (2017) where they used the same downscaling method. Equation 3.2 shows the procedure for the modified morphing method, which

can produce hourly future temperature data (T_{iF}) using the projected daily maximum and minimum values (T_{FMax} and T_{FMin}), as well as the available MERRA hourly historical data (T_{iB}).

$$T_{iF} = \frac{(T_{FMax} - T_{FMin})}{(T_{BMax} - T_{BMin})} \times (T_{iB} - T_{BMin}) + T_{FMin} \quad (3.2)$$

As seen from the above equation, the modified morphing method assumes that the minimum base hourly temperature gets translated to the minimum future hourly temperature; the same is assumed for the maximum base hourly temperature. For example, if historical data indicates that the minimum temperature on a given day occurred at 2 AM, then the modified morphing method assumes that the minimum temperature in the future will also occur at 2 AM. The same is the case with the maximum temperature. It should be noted that this approach may not be "strictly correct" as far as climate change is concerned. It is quite possible that the temperature distribution within a day will change in the future. Therefore, the times associated with minimum and maximum temperature may also change. However, modelling of such complex patterns was beyond the scope of this study, and therefore, the modified morphing approach was adopted in the current study for downscaling of the GCM-projected temperature data.

A MATLAB® script was developed to downscale the daily temperature data from all 20 GCM models using Equation 3.2 and generate the future hourly temperature distribution. The followings steps summarize the downscaling approach using the developed MATLAB® code:

1. Load historical MERRA climatic data and extract hourly historical temp data *(T_{iB})* for the 20-year period (for e.g., the historical period in this analysis was from 1985 till 2005);

2. Extract daily max *(T_{BMax})* and min *(T_{BMin})* values from the T_{iB} data, and calculate $(T_{BMax} - T_{BMin})$;
3. Load the GCM- projected climatic data (corresponding to RCP 4.5 or RCP 8.5 scenarios);
4. Extract daily max *(T_{FMax})* and min *(T_{FMin})* temperature data for the 20-year period of interest (the period of interest was set to 2046-2065 in the current study);
5. Convert the unit of temperature from Kelvin (K) to degree Fahrenheit (°F);
6. Calculate the difference between GCM-projected daily max and daily min temperatures $(T_{FMax} - T_{FMin})$;
7. Use Equation 3.2 to calculate the hourly future temperature data (T_{iF});
8. Replace the historical hourly temperature data (T_{iB}) with the downscaled future hourly temperature data (T_{iF});
9. Save the data as a new ".hcd" file for use with PMED.

Although the projected temperature data for all 20 GCMs corresponding to both RCP 4.5 and 8.5 scenarios were downscaled, only four (4) models were randomly selected in this study (see Table 3.11) for PMED simulations. The projected temperature distributions for all 20 GCMs were quite similar to each other, and the selection of four models out of 20 was sufficient for purposes of the current study. Two of the selected models were developed in the US, whereas one was developed in the United Kingdom (UK), and the fourth was developed in China. Note that for the sake of simplicity, the model ID (M1 through M4) has been used in the current document during the discussions.

Table 3.11 Global Climate Models (GCMs) Selected in the Current Study for Use with PMED

Model ID	Model Name	Developed by
M1	BNU-ESM	China
M2	CCSM4	USA
M3	GFDL-ESM2G	USA
M4	HadGEM2-ES365	UK

Figure 3.9 compares the temperature distributions projected by the four selected GCMs for Boise at the end of the design period (year 2065). From the boxplots in Figure 3.9 it can be seen that the median temperature values (indicated by the red horizontal lines) corresponding to the four models were very close to each other, and ranged between 50°F to around 55°F. The highest median value observed for Model M1. Similarly, a good correlation was observed between the 75^{th} and 25^{th} percentile temperature values from the four models. Besides, models M2 and M4 have wider range of projected temperature data compared to M1 and M3. Overall, no significant difference was observed between the projected temperature distributions from the four selected models.

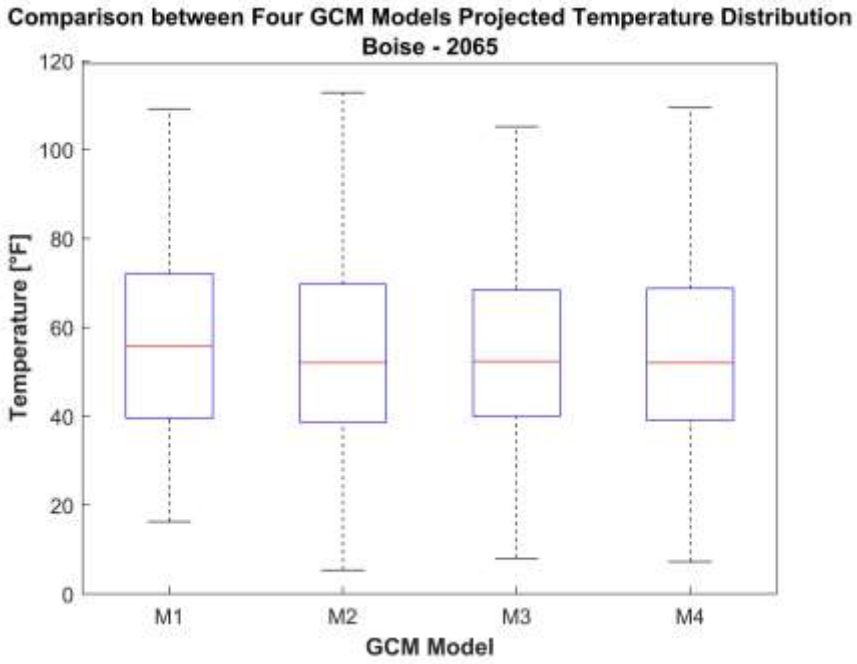

Figure 3.9 Comparison of Temperature Distributions Projected by the Four Selected GCMs for Boise in the Year 2065

Figure 3.9 clearly shows that the downscaled temperature data from the four selected models show a very high degree of correlation. For the sake of graphical representation, Figure 3.10 shows the projected temperature distribution for only one of the four models (M2-CCSM4) corresponding to the RCP 8.5 scenario. From Figure 3.10, the increase in frequencies corresponding to high temperatures in the Year 2065 can be observed for all three locations considered. This gives an idea of how temperature will be changing in the mid-21st century at the studied locations. It also clearly establishes that in the near future, pavement structures will be exposed to harsher temperature conditions. In light of this, the current practice of designing pavements assuming stationary climatic conditions is clearly inadequate.

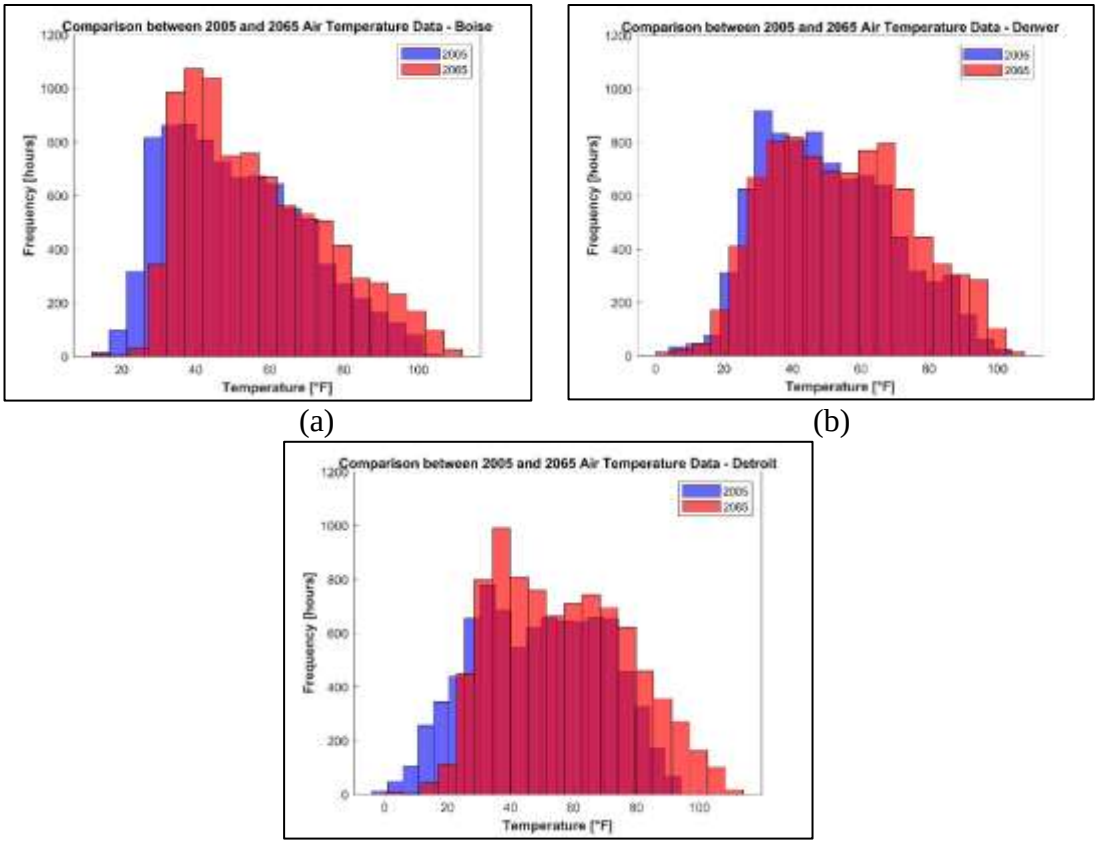

Figure 3.10 Comparison between the Temperature Frequency Distributions for Years 2005 and 2065 for: (a) Boise; (b) Denver; (c) Detroit

Usually, the air temperatures become warmer during summer months, and the resulting high pavement temperatures make them more susceptible to the temperature-sensitive distresses such as rutting. Although Figure 3.10 presented a picture of the overall temperature distribution for the two years being compared, a closer look at the temperature values on a smaller time scale would give a better idea regarding whether the temperatures are predicted to increase or decrease from 2005 to 2065. Accordingly, Figure 3.11 compares the summer temperatures in Boise, ID for the year 2005 (historical), and 2065; the future temperatures were projected using M2-CCSM4 for the RCP 8.5 scenario. Similar to the case for manual shifting (see Figure 3.1), the temperatures for the two years were compared at three different scales (hourly, weekly,

and monthly). Figure 3.11 confirms that the pavement will be exposed to higher temperatures during the summer of 2065 compared to what it was subjected to during the summer of 2005. Similar trends were observed for the two other cities (Denver and Detroit). However, the graphical representations of those trends have been excluded from the current chapter for the sake of brevity.

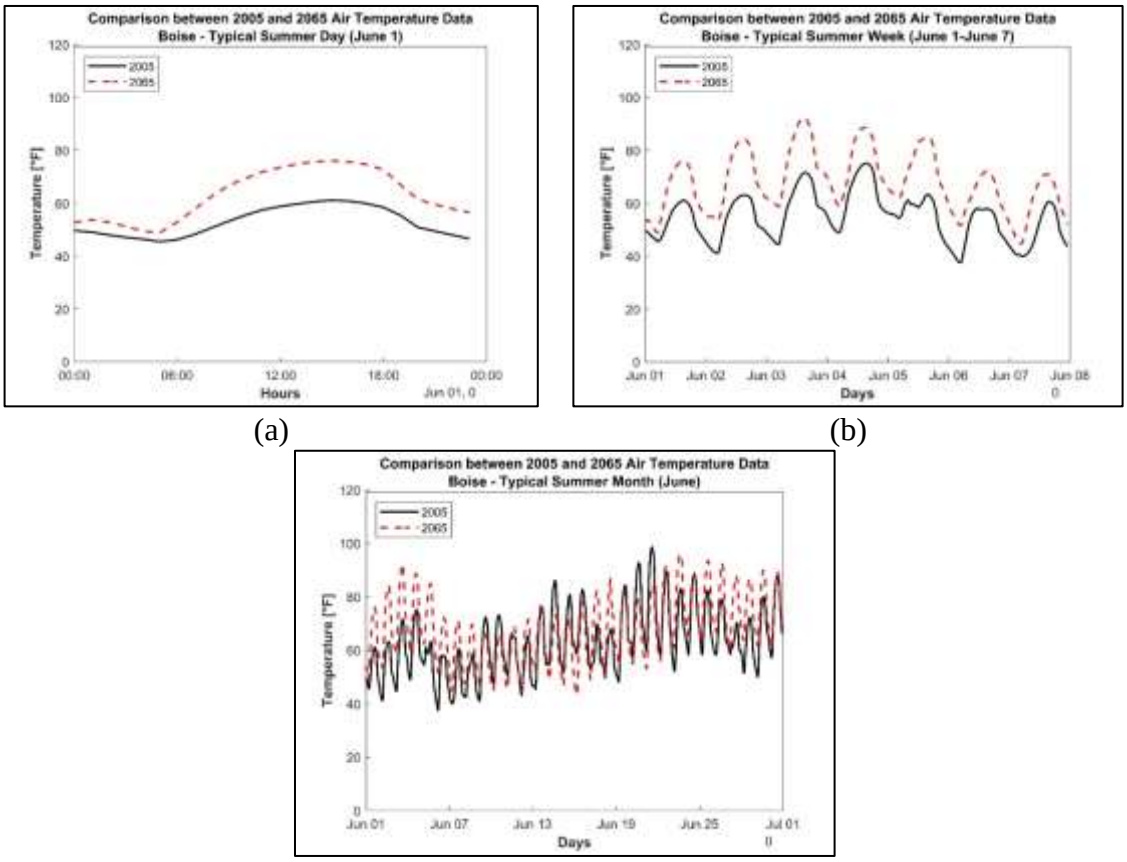

(a) (b)

(c)

Figure 3.11 Comparing the Temperatures for Boise in 2005 and 2065 at Different Time Scales: (a) Hours in a Day; (b) Days in a Week; (c) Days in a Month

Analysis of Temperature Sensitivity of PMED Distress Predictions using GCM-Projected Data

Comparison Between Historical and GCM-Projected Cases: Multiple Cities

Similar to the case of manual shifting of temperature distribution, the GCM-projected temperature distributions were also taken for three different locations (Boise, Denver, and Detroit), and corresponding PMED simulations were run to compare the pavement performance predictions. As already mentioned, only four (4) GCM models were used for this purpose. The analyses were performed between the time periods 2046 to 2065 for both RCP 4.5 and RCP 8.5 scenarios.

Table 3.12 compares the simulation results obtained for the historical and GCM-projected temperature distribution scenarios. Just like the case for manual shifting, the results for Boise seem to have a very low sensitivity to temperature change in terms of AC rutting prediction. In contrast, with almost similar temperature conditions, Denver shows very high sensitivity to the temperature change at the end of the design life. Besides, for some projected cases of Detroit, the thermal cracking increases with an increase in temperature, which is definitely related to the pavement cooling rate and tensile strength of asphalt mix.

Overall, the comparison of simulation results for RCP 4.5 and RCP 8.5 from Tables 3.12 clearly shows that the RCP 8.5 scenario has a higher impact on distress prediction than RCP 4.5 due to its extreme projection of temperature change. Finally, three of the GCMs were found to have a similar impact on pavement distress predictions except for Model 4, which showed the highest distresses.

Table 3.12 Summary of multiple cities GCM projected LCFs simulations results

Model	Total Pavement Rutting (in.)			AC Rutting (in)			AC Thermal Cracking (ft/mile)		
	BOI	**DEN**	**DTM**	**BOI**	**DEN**	**DTM**	**BOI**	**DEN**	**DTM**
Historical									
MERRA	0.37	0.75	0.32	0.13	0.42	0.29	721.90	2592.57	175.13
Projected- RCP 4.5									
M1	0.38	0.82	0.42	0.14	0.49	0.40	216.20	2592.57	175.12
M2	0.38	0.83	0.41	0.14	0.49	0.39	217.29	2592.57	175.12
M3	0.38	0.80	0.40	0.14	0.47	0.37	350.67	2592.57	175.12
M4	0.39	0.86	0.47	0.15	0.53	0.44	175.13	2592.57	356.50
Projected- RCP 8.5									
M1	0.39	0.84	0.46	0.15	0.51	0.43	383.92	2592.57	356.50
M2	0.38	0.84	0.45	0.15	0.51	0.42	175.12	2592.57	175.12
M3	0.38	0.83	0.41	0.14	0.50	0.39	175.17	2592.57	175.12
M4	0.40	0.90	0.53	0.16	0.57	0.50	356.50	2773.95	356.50

Effect of LCFs on PMED Rutting Predictions due to GCM-Projected Temperature Distributions

Just like the case for manual shifting of temperature distributions, the following three PMED GCM scenarios were simulated to evaluate the effect of LCFs on PMED rutting prediction.

1. Use the GCM-projected climatic data for Boise with LCFs from the three different states (ID, CO, MI)

2. Use the GCM-projected climatic data for Denver with LCFs from the three different states (ID, CO, MI)
3. Use the GCM-projected climatic data for Detroit with LCFs from the three different states (ID, CO, MI)

Projected temperature data for two of the GCMs (M2 and M4) under RCP 8.5 projected scenario were considered for the LCFs analysis. Table 3.13 summarizes the predicted rutting results from all the PMED simulations. Results confirm a similar trend, which was observed from the manual shifting simulations. As previously observed, the LCFs for Idaho were relatively insensitive to temperature increases while predicting pavement performance.

Table 3.13 Summary of Simulation Results obtained from Different LCFs and Same GCMs Climatic Data

Climatic Condition	Model	Total Pavement Rutting (in.)			AC Rutting (in)		
		State LCF					
		ID	MI	CO	ID	MI	CO
		GCM-Projected Climatic Data for BOI					
Historical	MERRA	0.37	0.78	0.44	0.13	0.45	0.42
Projected-RCP 8.5	M2	0.38	0.84	0.51	0.15	0.52	0.48
	M4	0.40	0.90	0.57	0.16	0.58	0.55
		GCM-Projected Climatic Data for DEN					
Historical	MERRA	0.36	0.75	0.41	0.12	0.42	0.38
Projected-RCP 8.5	M2	0.38	0.84	0.50	0.14	0.51	0.47
	M4	0.40	0.90	0.56	0.16	0.57	0.54
		GCM-Projected Climatic Data for DTM					
Historical	MERRA	0.34	0.68	0.32	0.09	0.33	0.29
Projected-RCP 8.5	M2	0.37	0.80	0.45	0.13	0.47	0.42
	M4	0.39	0.87	0.53	0.15	0.54	0.50

CHAPTER FOUR: SUMMARY, FINDINGS, AND RECOMMENDATIONS FOR FUTURE RESEARCH

Summary and Findings

This research study primarily focused on investigating how the Mechanistic-Empirical Pavement Design approach implemented into AASHTOWare Pavement ME Design (PMED) accommodates the effect of climate change on flexible pavement performance. Only the effects of temperature change on flexible pavement performance was studied. Temperature distributions for the future were generated using two different approaches: (1) manual shifting of the historical temperature distribution, and (2) downscaling of temperature distributions projected by established global climatic models (GCMs). PMED simulations were run for the different temperature distribution scenarios, and the performance predictions were compared against the base case (where the historical temperature distribution was used assuming stationary climatic conditions). Initial analysis was performed only for Boise, ID, using both the Global Calibration Factors (GCFs) and Local Calibration Factors (LCFs). However, subsequent analysis was done by considering two more study locations, i.e., Denver, Colorado, and Detroit, Michigan. A comparative analysis of the predicted parameters for three states and different climatic scenarios were conducted to identify the variability in distress predictions due to different geographic conditions. Besides, this study also extensively analyzed the transfer functions of PMED performance models and the effect of Local Calibration Factors (LCF's) in predicting the temperature sensitivity. Moreover, PMED-

generated intermediate files were analyzed to study the impact of air temperature on pavement temperature and AC layer modulus at the end of the design life.

The major findings of this study are as follows:

1. The effect of changing air temperatures can be different for pavements constructed in different parts of the country.
2. Temperature change was found to have no significant effect on bottom-up fatigue cracking predictions.
3. Rutting and thermal cracking predictions vary significantly based on the LCFs used by different state highway agencies.
4. LCFs established for Idaho, were the least sensitive in capturing the effect of temperature change on flexible pavement performance. This was directly attributed to the low value of $\beta 3$ (temperature exponent) established for Idaho through the local calibration effort.
5. Colorado's LCF's were found to have a very high sensitivity to the temperature change in predicting the pavement distresses. Once again, this was attributed to the highest value of $\beta 3$ among the three locations being compared.
6. Analysis of monthly quintile temperature and hourly temperature of the pavement AC layer as well as sublayer AC modulus showed expected trends due to changes in projected air temperatures. As the air temperature increased, the AC layer temperature increased, and the AC sublayer moduli decreased.
7. Simulations results for some projected scenarios indicated an increase in thermal cracking due to the increased temperatures. This was attributed to

high cooling rate of the pavement surface as well as reduced asphalt tensile strength at higher temperatures. However, inconsistent thermal cracking trends were also observed for some of the scenarios

8. PMED simulations using GCM-projected temperature data confirmed all the observations made through the manual shifting

Recommendation for Future Research

Based on the research findings and knowledge gained from the different research tasks, the following recommendations for future research can be made:

1. This study considered a new (hypothetical) pavement section for studying the temperature sensitivity of predicted performance. In future research, considering an existing pavement section at the studied location(s) would produce more realistic results.
2. Similar analyses should be conducted on pavement sections with different AC layer thicknesses and material properties to assess how variations in the pavement structure and material properties affect the temperature sensitivity.
3. The current study only focused on temperature changes while studying the effects of climate change on flexible pavement performance. Similar studies should be carried out to study the effects of precipitation as well as percent sunshine. Also, a separate study is required to study the effects of climate change on rigid pavement performance.
4. Findings from this study indicated that the LCFs established for Idaho were relatively insensitive to temperature changes. This aspect should be further

investigated, and if necessary, some of the LCFs used in Idaho should be updated.

REFERENCES

AASHTOWare® DARWin-ME™. American Association of State Highway and Transportation Officials, Washington, D.C.

Abatzoglou J.T., & Brown T.J. (2012). A comparison of statistical downscaling methods suited for wildfire applications, International Journal of Climatology. 32, 772-780.

Allen, M. R., Dube, O. P., Solecki, W., Aragon-Durand, F., Cramer, W., Humphreys, S., & Zickfeld, K. (2018). Framing and Context "in Global Warming of 1.5 C: An IPCC Special Report on the impacts of global warming of 1.5 C above pre-industrial levels and related global greenhouse gas emission pathways, in the context of strengthening the global response to the threat of climate change, sustainable development, and efforts to eradicate poverty.

American Association of State Highway and Transportation Officials (AASHTO) (2008). Mechanistic-Empirical Pavement Design Guide, Interim Edition, a Manual of Practice.

American Association of State Highway and Transportation Officials (AASHTO) (2010). Guide for the Local Calibration of the Mechanistic-Empirical Pavement Design Guide. Washington, DC: American Association of State Highway and Transportation Officials.

American Association of State Highway and Transportation Officials (AASHTO) (2019). AASHTOWare® Pavement ME Design™ software (formerly

American Association of State Highway and Transportation Officials (AASHTO) (2020). Mechanistic-Empirical Pavement Design Guide, Third Edition, a Manual of Practice. Washington, DC: American Association of State Highway and Transportation Officials.

Apeagyei, A. K., Dave, E. V., & Buttlar, W. G. (2008). Effect of cooling rate on thermal cracking of asphalt concrete pavements. Asphalt Paving Technology-Proceedings, 77, 709.

Applied Research Associates (ARA) (2004). Guide for the Mechanistic-Empirical Design of New & Rehabilitated Pavement Structures. NCHRP Project 1-37A. Transportation Research Board, Washington, DC.

Bayomy, F., El-Badawy, S., & Awed, A. (2012). Implementation of the MEPDG for flexible pavements in Idaho (No. FHWA-ID-12-193). Idaho. Transportation Dept..

Bayomy, F., Muftah, A., & Kassem, E. (2018). Calibration of the AASHTOWare Pavement ME Design Performance Models for Flexible Pavements in Idaho. (No. FHWA-ID/18-235). Idaho. Transportation Dept..

Belcher, S.E., Hacker, J.N., & Powell, D.S., (2005). Constructing design weather data for future climates. Build. Serv. Eng. Res. Technol. 26 (1), 49–61.

Bureau of Transportation Statistics (BTS) (n.d.). National Transportation Statistics. https://www.bts.gov/topics/national-transportation-statistics.

Central Intelligence Agency (CIA) (n.d.). The CIA world factbook. Retrieved November 17, 2019, from https://www.cia.gov/library/publications/resources/the-world-factbook

Climate change. (n.d.). In Wikipedia. Retrieved November 17, 2019, from https://simple.wikipedia.org/wiki/Climate_change#:~:text=Climate%20change%20is%20any%20significant,other%20parts%20of%20the%20Earth.

Daniel, J. S., Jacobs, J. M., Douglas, E., Mallick, R. B., & Hayhoe, K. (2014). Impact of climate change on pavement performance: Preliminary lessons learned through the infrastructure and climate network (ICNet). In Climatic Effects on Pavement and Geotechnical Infrastructure (pp. 1-9).

Daniel, J. S., Jacobs, J. M., Miller, H., Stoner, A., Crowley, J., Khalkhali, M., & Thomas, A. (2018). Climate change: potential impacts on frost–thaw conditions and

seasonal load restriction timing for low-volume roadways. Road Materials and Pavement Design, 19(5), 1126-1146.

Darter, M. I., Mallela, J., Titus-Glover, L., Rao, C., Larson, G., Gotlif, A., & El-Badawy, S. M. (2006). Changes to the" Mechanistic-Empirical Pavement Design Guide" Software Through Version 0.900, July 2006. NCHRP Research Results Digest, (308).

Darter, M. I., Titus-Glover, L., & Von Quintus, H. L. (2009). Implementation of the mechanistic-empirical pavement design guide in Utah: Validation, calibration, and development of the UDOT MEPDG user's guide (No. UT-09.11). Utah. Dept. of Transportation. Research Division.

Douglas, E., Jacobs, J., Hayhoe, K., Silka, L., Daniel, J., Collins, M., Mallick, R. (2017). Progress and challenges in incorporating climate change information into transportation research and design. Journal of Infrastructure Systems, 23(4), 04017018

Elshaeb, M. A., El-Badawy, S. M., & Shawaly, E. S. A. (2014). Development and impact of the Egyptian climatic conditions on flexible pavement performance. American Journal of Civil Engineering and Architecture, 2(3), 115-121.

El-Maaty, A. E. A. (2017). Temperature change implications for flexible pavement performance and life. International Journal of Transportation Engineering and Technology, 3(1), 1-11.

Federal Highway Administration (FHWA) (n.d.). Long-Term Pavement Performance (LTPP) program. LTPPInfoPave -Tools: MERRA Climate Data for MEPDG input. Retrieved June 26, 2020, from https://infopave.fhwa.dot.gov/Tools/MEPDGInputsFromMERRA.

Federal Highway Administration (FHWA) (n.d.). Long-Term Pavement Performance (LTPP) program. LTPPInfoPave-Tools: LTPPBind online. Retrieved June 26, 2020, from https://infopave.fhwa.dot.gov /Tools/LTPPBindOnline.

Generalized extreme value distribution. (n.d.). In Wikipedia. Retrieved November 17, 2019, from https://en.wikipedia.org/wiki/Generalized_extreme_value_distribution

Gudipudi, P. P., Underwood, B. S., & Zalghout, A. (2017). Impact of climate change on pavement structural performance in the United States. Transportation Research Part D: Transport and Environment, 57, 172-184.

Haider, S. W., Buch, N., Brink, W., Chatti, K., & Baladi, G. (2014). Preparation for implementation of the mechanistic-empirical pavement design guide in Michigan, part 3: local calibration and validation of the pavement-ME performance models (No. RC-1595). Michigan. Dept. of Transportation. Office of Research Administration.

Hall, K. D., & Beam, S. (2005). Estimating the sensitivity of design input variables for rigid pavement analysis with a mechanistic-empirical design guide. Transportation Research Record, 1919(1), 65-73.

Hansen, J., Sato, M., & Ruedy, R. (2012). Perception of climate change. Proceedings of the National Academy of Sciences, 109(37), E2415-E2423.

Hasan, M. A., & Tarefder, R. A. (2018). Development of temperature zone map for mechanistic-empirical (ME) pavement design. International Journal of Pavement Research and Technology, 11(1), 99-111.

Hayhoe, K., Stoner, A., Abeysundara, S., Daniel, J. S., Jacobs, J. M., Kirshen, P., & Benestad, R. (2015). Climate projections for transportation infrastructure planning, operations and maintenance, and design. Transportation Research Record, 2510(1), 90-97.

Hayhoe, K., Wake, C., Anderson, B., Liang, X. Z., Maurer, E., Zhu, J., & Wuebbles, D. (2008). Regional climate change projections for the Northeast USA. Mitigation and Adaptation Strategies for Global Change, 13(5-6), 425-436.

Huang, Y. H., (2004). Pavement Analysis and Design. 2nd edn. New Jersey: Pearson Prentice Hall.

Jibon, M., Mishra, D., & Kassem, E. (2020). Laboratory Characterization of Fine-Grained Soils for Pavement ME Design Implementation in Idaho.Transportation Geotechnics, 100395.

Knott, J. F., Elshaer, M., Daniel, J. S., Jacobs, J. M., Kirshen, P. (2017). Assessing the effects of rising groundwater from sea level rise on the service life of pavements in coastal road infrastructure. Transportation Research Record, 2639(1), 1-10.

Larson, G., & Dempsey, B. J. (1997). Enhanced integrated climatic model Version 2.0. Department of Civil and Environmental Engineering.

Li, Q. J., Wang, K. C., Nguyen, V., & "Doc" Zhang, Z. (2013). Validation of TMG Traffic Data Check Algorithms. Journal of transportation engineering, 139(11), 1141-1145.

Lytton, R. L., Luo, X., Ling, M., Chen, Y., Hu, S., & Gu, F. (2018). A Mechanistic–Empirical Model for Top–Down Cracking of Asphalt Pavements Layers (No. NCHRP Project 01-52).

Mallela, J., Titus-Glover, L., Bhattacharya, B., Darter, M., & Von Quintus, H. (2014). Idaho AASHTOWare pavement ME design user's guide, version 1.1 (No. FHWA-ID/14-211B). Idaho. Transportation Dept..

Mallela, J., Titus-Glover, L., Sadasivam, S., Bhattacharya, B., Darter, M., & Von Quintus, H. (2013). Implementation of the AASHTO mechanistic-empirical pavement design guide for Colorado (No. CDOT-2013-4). Colorado. Dept. of Transportation. Research Branch.

Mallick, R. B., Jacobs, J. M., Miller, B. J., Daniel, J. S., & Kirshen, P. (2018). Understanding the impact of climate change on pavements with CMIP5, system dynamics and simulation. International Journal of Pavement Engineering, 19(8), 697-705.

MATLAB version 2019b (2019). The MathWorks, Inc. https://www.mathworks.com/products/matlab.html.

National Aeronautics and Space Administration (NASA) (2009). Modern-Era Retrospective analysis for Research and Applications (MERRA). Retrieved November June 26, 2020, from https://gmao.gsfc.nasa.gov/reanalysis/MERRA/.

National Aeronautics and Space Administration (NASA) (2014, May 14). What Is Climate Change? Retrieved November 17, 2019, from https://www.nasa.gov/audience/forstudents/k-4/stories/nasa-knows/what-is-climate-change-k4.html.

National Aeronautics and Space Administration (NASA) (n.d.). NASA Climate Change: How Do We Know? Retrieved November 17, 2019 from https://climate.nasa.gov/evidence/

Pachauri, R. K., Allen, M. R., Barros, V. R., Broome, J., Cramer, W., Christ, R., & Dubash, N. K. (2014). Climate change 2014: synthesis report. Contribution of Working Groups I, II and III to the fifth assessment report of the Intergovernmental Panel on Climate Change (IPCC). (p. 151).

Qiao, Y., Dave, E., Parry, T., Valle, O., Mi, L., Ni, G., & Zhu, Y. (2019). Life Cycle Costs Analysis of Reclaimed Asphalt Pavement (RAP) Under Future Climate. Sustainability. 11(19), 5414.

Qiao, Y., Flintsch, G. W., Dawson, A. R., & Parry, T. (2013). Examining effects of climatic factors on flexible pavement performance and service life. Transportation research record, 2349(1), 100-107.

Schwartz, C. W., Forman, B. A., & Leininger, C. W. (2015). Alternative source of climate data for mechanistic-empirical pavement performance prediction. Transportation Research Record, 2524(1), 83-91.

Stocker, T. F., Qin, D., Plattner, G. K., Tignor, M., Allen, S. K., Boschung, J., & Midgley, P. M. (2013). Climate change 2013: The physical science basis. Contribution of working group I to the fifth assessment report of the intergovernmental panel on climate change, 1535.

Stoner, A. M., Daniel, J. S., Jacobs, J. M., Hayhoe, K., & Scott-Fleming, I. (2019). Quantifying the impact of climate change on flexible pavement performance and life-time in the United States. Transportation Research Record, 2673(1), 110-122.

Taylor, K. E., Stouffer, R. J., & Meehl, G. A. (2012). An Overview of CMIP5 and the Experiment Design. Bull. Amer. Meteor. Soc., 93, 485 - 498, https://doi.org/10.1175/BAMS-D-11-00094.1.

Underwood, B. S., Guido, Z., Gudipudi, P., Feinberg, Y. (2017). Increased costs to US pavement infrastructure from future temperature rise. Nature Climate Change, 7(10), 704.

United States Environmental Protection Agency (EPA) (n.d.). Climate Impacts in the Northwest Retrieved August 2, 2020, from https://19january2017snapshot.epa.gov/ climate-impacts/climate-impacts-northwest_.html

Yang, X., You, Z., Hiller, J., & Watkins, D. (2017). Sensitivity of flexible pavement design to Michigan's climatic inputs using pavement ME design. International Journal of Pavement Engineering, 18(7), 622-632.